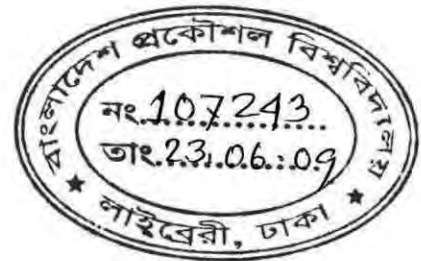
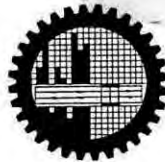
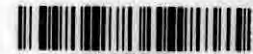


Determination of Relative Density of Sand Using Dynamic Cone Resistance Data



by

Mohammad Shahadat Hossain



A project submitted to the Department of Civil Engineering,
Bangladesh University of Engineering and Technology,
Dhaka, in partial fulfillment of the degree of

MASTER OF ENGINEERING (Civil and Geotechnical)
DEPARTMENT OF CIVIL ENGINEERING
BANGLADESH UNIVERSITY OF ENGINEERING AND TECHNOLOGY,
DHAKA

2009

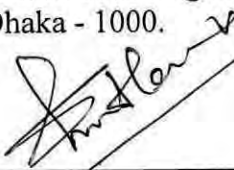
The project titled "**Determination of Relative Density of Sand Using Dynamic Cone Resistance Data**" Submitted by **Mohammad Shahadat Hossain**, Roll No. **100604221(P)**, Session **2006**, has been accepted as satisfactory in partial fulfillment of the requirement for the degree of **Master of Engineering (Civil and Geotechnical)** on **May 17, 2009**.

BOARD OF EXAMINERS



Dr. Md. Jahangir Alam
Assistant Professor
Department of Civil Engineering
BUET, Dhaka - 1000.

Chairman
(Supervisor)



Dr. Md. Saiful Alam Siddique
Professor
Department of Civil Engineering
BUET, Dhaka - 1000.

Member



Dr. Mohammad Shariful Islam
Associate Professor
Department of Civil Engineering,
BUET, Dhaka-1000.

Member

CANDIDATE'S DECLARATION

It is hereby declared that this thesis or any part of it has not been submitted elsewhere for the award of any degree or diploma.



(Mohammad Shahadat Hossain)

Table of Contents

CANDIDATE'S DECLARATION.....	iii
Table of Contents.....	iv
List of Figures.....	vi
List of Tables.....	ix
NOTATIONS.....	x
Acknowledgement.....	xi
Abstract.....	xii
Chapter 1: INTRODUCTION.....	1
1.1 General.....	1
1.2 Background of the Study.....	2
1.3 Objectives of the Study.....	3
1.4 Methodology.....	3
1.5 Organization of the Thesis.....	4
Chapter 2: LITERATURE REVIEW.....	5
2.1 Introduction.....	5
2.2 General Principle of Dynamic Probing.....	5
2.3 Various types of Dynamic Probing.....	5
2.4 Specification of Dynamic Probing Light (DPL).....	6
2.5 DCP.....	7
2.5.1 History of DCP.....	8
2.5.2 Parts of DCP.....	9
2.5.3 Correlations with DCP.....	10
2.5.4 Application of Dynamic Cone Penetrometer (DCP).....	12
Chapter 3: TESTING PROGRAM.....	22
3.1 Introduction.....	22
3.2 Calibration of Air Pluviation Method.....	22

3.3	DCP and DPL Tests in Calibration Chamber	23
3.3.1	Preparation of Sand Deposit in Calibration Chamber.....	23
3.3.2	Tests in Calibration Chamber	23
Chapter 4: RESULTS AND DISCUSSION		36
4.1	Introduction.....	36
4.2	Calibration of Air Pluviation Method	36
4.3	Result of DCP and DPL in Calibration Chamber	36
4.3.1	Determination of P_{index} and N_{10}	37
4.3.2	Development of Correlation between Relative Density and P_{index}	37
4.4	Verification of Correlation from Field Data	38
4.5	Findings.....	40
Chapter 5: CONCLUSIONS.....		51
5.1	General.....	51
5.2	Conclusions.....	51
5.3	Recommendations for Future Study	52
REFERENCES		53
Appendix A:		58
DCP & DPL TEST RESULTS		58
Appendix B:		72
ASTM Standard of DCP		72

List of Figures

- Fig. 2.1:** Schematic diagram of Dynamic Probing Light (DPL)
- Fig. 2.2:** The dimensions of 6 kg anvil of DPL
- Fig. 2.3:** Dimensions of 10 kg hammer of DPL
- Fig. 2.4:** Dimension of Probing cone of DPL
- Fig. 2.5:** Schematic diagram of Dynamic Cone Penetration (DCP) test
- Fig. 2.6:** Different dimensions of probing cone of DCP
- Fig. 2.7:** Different dimensions of Anvil of DCP
- Fig. 2.8:** Dimensions of 8 kg hammer of DCP
- Fig. 2.9:** Handle to hold DCP during test
- Fig. 2.10:** Plot of Standard Penetration value vs Penetration Index (Tom Burnham, 1993)
- Fig. 2.11:** Plot of California Bearing Ratio, Unconfined Compression Strength vs Penetration Index (Tom Burnham, 1993)
- Fig. 2.12:** The weak spot in sub grade bridge embankment. (Tom Burnham, 1993)
- Fig. 3.1:** General view of multiple sieving pluviation apparatus (Miura and Toki, 1982)
- Fig. 3.2:** Sand discharge bowl with 4 mm diameter holes
- Fig. 3.3:** Spacing and pattern of holes of discharge bowls.
- Fig. 3.4:** Air pluviation method
- Fig. 3.5:** Grain size distribution of fine sand and medium sand used in the study
- Fig. 3.6:** Calibration chamber and working platform
- Fig. 3.7:** Calibration chamber surrounded by thick polythene sheet to minimize disturbance by wind
- Fig. 3.8:** Drying of sand before test
- Fig. 3.9:** Dry deposition into calibration chamber from discharging bowl maintaining a constant height of fall
- Fig. 3.10:** Recharging of discharge bowl

- Fig. 3.11:** Filling of calibration chamber in progress
- Fig. 3.12:** Densification of sand into calibration chamber using concrete vibrator
- Fig. 3.13:** Initial reading of the scale before starting DCP
- Fig. 4.1:** Relative Density vs height of fall for fine sand
- Fig. 4.2:** Relative Density vs height of fall for medium sand
- Fig. 4.3:** Typical plot of number of blows vs depth (DCP) plot for fine sand in calibration chamber
- Fig. 4.4:** Typical plot of number of blows vs depth (DPL) plot for fine sand in calibration chamber
- Fig. 4.5:** Typical plot of number of blows vs depth (DCP) for medium sand in calibration chamber
- Fig. 4.6:** Typical plot of number of blows vs depth (DPL) for medium sand in calibration chamber
- Fig. 4.7:** Typical plot of number of blows vs depth (DCP) for fine sand in calibration chamber (Vibration method)
- Fig. 4.8:** Typical plot of number of blows vs depth (DPL) for fine sand in calibration chamber (Vibration method)
- Fig. 4.9:** Correlation between Relative Density and $P_{\text{index}}\sqrt{D_{50}}$ in DCP for any sand (Linear scale)
- Fig. 4.10:** Correlation between Relative Density and $P_{\text{index}}\sqrt{D_{50}}$ in DPL for any sand (Linear scale)
- Fig. 4.11:** Typical plot of number of blows vs depth of DPL test in Pangaon Site
- Fig. 4.12:** Typical plot of Penetration Index vs depth of DPL test in Pangaon Site
- Fig. 4.13:** Typical plot of Relative Density vs depth obtained from DPL test in Pangaon Site
- Fig. 4.14:** Comparison of Relative Density obtained from DCP and DPL test and Sand Cone Method before introduction of correction factor
- Fig. 4.15:** Comparison of Relative Density obtained from DCP test and Sand Cone Method after introduction of correction factor
- Fig. 4.16:** Comparison of Relative Density obtained from DPL test and Sand

Cone Method after introduction of correction factor

- Fig. 4.17:** Relative Density vs depth obtained from DCP, DPL and Sand Cone Method (Location 1, Point 1, Jamuna site)
- Fig. 4.18:** Relative Density vs depth obtained from DCP, DPL and Sand Cone Method (Location 2, Point 1, Jamuna site)
- Fig. 4.19:** Relative Density vs depth obtained from DCP, DPL and Sand Cone Method (Location 1, Point 1, Pangaon site)
- Fig. 4.20:** Relative Density vs depth obtained from DCP, DPL and Sand Cone Method (Location 2, Point 1, Pangaon site)

List of Tables

- Table 2.1:** Technical data of the equipment used in Dynamic Probing
- Table 2.2:** Specification of Dynamic Probing Light
- Table 2.3:** Developed correlation of DCP with CBR (Amini, 2003)
- Table 3.1:** Properties of two types of sand
- Table 3.2:** Calibration of air pluviation method for fine sand (Opening of discharging bowl 3.5 mm)
- Table 3.3:** Calibration of air pluviation method for fine sand (Opening of discharging bowl 4.0 mm)
- Table 3.4:** Calibration of air pluviation method for medium sand (Opening of discharging bowl 4.0 mm)
- Table 3.5:** Calibration of air pluviation method for medium sand (Opening of discharging bowl 5.0 mm)
- Table 3.6:** Basic differences between DCP and DPL
- Table 4.1:** Generalized correlation between Relative Density and $P_{\text{index}}*\sqrt{(D_{50})}$ for all types of clean sand.

NOTATIONS

- CBR = California Bearing Ratio;
- CPT = Cone penetration test;
- DCP = Dynamic cone penetrometer;
- DP = Dynamic probing;
- DPL = Dynamic probing light;
- g = Acceleration of gravity;
- H = Height of fall;
- M = Mass of hammer;
- MS = Mild steel;
- MSP = Multiple sieving pluviation;
- N_{10} = Number of blow required for 10 cm penetration of cone;
- P_{index} = Penetration Index (rate of penetration in mm/blow);
- D_r = Relative Density;
- SS = Stainless steel;
- SPT = Standard penetration test;
- γ_{max} = Maximum index dry density;
- γ_{min} = Minimum index dry density;
- γ_d = Field dry density;

Acknowledgement

The author wishes to express his deep appreciation to the almighty Allah for allowing him to bring an end of this thesis. Then he desires to convey his admiration to his supervisor Dr. Md Jahangir Alam, Assistant Professor, Department of Civil Engineering, Bangladesh University of Engineering and Technology (BUET), for his keen interest, valuable suggestions, proper guidance, cordial association and supervision throughout the project work. In the different stages of study and report making, his appropriate opinion and suggestions helped to avoid omissions, confusions and inconsistency.

The author gratefully acknowledges the construction criticisms and valuable suggestions made by Professor Dr. Md. Saiful Alam Siddiquee and Associate Professor Dr. Mohammad Shariful Islam. Thanks are extended to Mr. Ziaur Rahman who started to develop this correlation as a part of his undergraduate thesis and Mr. Abul kalam Azad who made a correlation between Relative Density and N_{10} for Sylhet sand and Jamuna sand using DCP and DPL in his M.Sc.Engg. thesis. Thanks are also extended to Mr. Shahabuddin and Mr. Khokon from geotechnical lab for there helps and assistance during experimental works.

Abstract

Sand fill beneath the structure and surrounding area should be well compacted to make it non liquefiable. Once a structure is constructed on liquefiable soil, mitigation measures become very expensive. Therefore, it is very important to control the quality of sand fill so that structure would not be vulnerable to damage induced by seismic liquefaction. Compaction control of sand fill is generally done by determining field density using Sand Cone Method in Bangladesh. Sand Cone Method is expensive and cumbersome to do after completion of compaction in every single layer. The present study was aimed at developing an alternative indirect method which can be used to determine Relative Density easier and faster for clean sand of any particle size.

The study consists of three stages. To know the height of fall and hole diameter of sand discharging bowl for a desired Relative Density of a specific sand, the air pluviation method was calibrated in the first stage. Then in the second stage sand deposits of different relative densities were prepared in calibration chamber and Dynamic Probing Light (DPL) and Dynamic Cone Penetrometer (DCP) tests were performed on the prepared sand deposit. Correlation between Penetration Index (rate of penetration in mm/blow, P_{index}) and Relative Density was made from the test results in calibration chamber. At the last stage, the correlation was verified for two dredge fill sites where DCP and DPL results were compared with the result from Sand Cone Method.

A generalized correlation between P_{index} and Relative Density for clean sand of any particle size was found from this study. To determine in situ Relative Density of sand deposit, it is concluded that the proposed method (DCP and DPL) can be used as an alternative indirect method which is suitable up to 2 m depth.

CHAPTER 1 INTRODUCTION



1.1 General

The density of granular soils varies with the shape and size of grains, the gradation and the manner in which the mass is compacted. The term used to indicate the strength characteristics in a qualitative manner is Relative Density (D_r) (Murthy, 1993) which describes the state condition in cohesionless soils. It is commonly used to identify liquefaction potential under earthquake or other shock-type loading (Seed and Idris, 1971). So Relative Density is a very important index for a sandy soil. Relative Density is 0% for loosest condition of sand and 100% for densest condition of sand. If maximum index density and minimum index density of sand is determined in laboratory as per ASTM D4253 and D4254, and field dry density is determined by any one of the methods such as Sand Cone Method (ASTM D1556), Sleeve Method (ASTM D4564), Rubber Balloon Method (ASTM D2167), and Drive-Cylinder Method (ASTM D2937), Relative Density can be calculated using the following formula.

$$D_r = \left(\frac{\gamma_d - \gamma_{\min}}{\gamma_{\max} - \gamma_{\min}} \right) \left(\frac{\gamma_{\max}}{\gamma_d} \right) \cdot 100 \text{-----1.1}$$

Where,

γ_d = field dry density of sand deposit

γ_{\max} = maximum index density

γ_{\min} = minimum index density.

Relative Density can be expressed in terms of void ratio as follows:

$$D_r(\%) = \left(\frac{e_{\max} - e}{e_{\max} - e_{\min}} \right) \cdot 100 \text{-----1.2}$$

Where, e_{\max} = Maximum possible void ratio

e_{\min} = Minimum possible void ratio

e = void ratio in natural state of soil

Sand fill are required for many purposes, for example, backfill of earth retaining structures, backfill in foundation trenches, reclamation of low lands etc. In all these situations good compaction of fill should be ensured to avoid future subsidence, failure of foundation and moreover liquefaction. Relative Density is the most appropriate index to control the compaction of sand fill. Depending on the importance of structure, minimum Relative Density generally be specified as 70% to 95%.

1.2 Background of the Study

To develop low lands, dredge fill sand is usually used which meet the need of growing people to construct many facilities like model towns, inland container terminal, deep sea-port etc. It is proved that dredge fill sand is liquefiable from several case studies of earthquakes. In earthquake when seismic liquefaction occurs, even pile foundations could not save the structure from damage in many cases. To make the sand fill non liquefiable it should be well compacted. Mitigation measures become very expensive if a structure is constructed on liquefiable soil and it would be damaged during earthquake. So, it is very important to control the quality of sand fill.

In our country, quality control of sand fill is done by determining field density near the top surface of fill using Sand Cone Method (ASTM D 1556-90, 2006). It has limitations because it is a direct method of determining field density and Relative Density of sand fill. This method is very difficult to perform at deeper locations. Sand Cone Method has to be applied to control the quality of sand fill after compaction/densification of each layer of fill. For this reason it is time consuming and expensive to use Sand Cone Method. Sand Cone Method can not be applied in saturated sand or where water table is high. To determine Relative Density of sand fill easily, it is necessary to develop an indirect method which can be performed in all seasons and in any location. Azad (2008) proposed Dynamic Cone Penetrometer

(DCP) and Dynamic Probing Light (DPL) as indirect method of determining Relative Density of sand fill. He established correlations between Relative Density and N_{10} (number of hammer blows required for 10 cm penetration of cone) of DCP and DPL for Jamuna sand and Sylhet sand. Finally, he established generalized correlation for any size of sand. Now it is necessary to calibrate DCP and DPL for other sands which have different grain size distribution and mean diameter to verify generalized correlation of Azad (2008).

1.3 Objectives of the Study

The present study has the following objectives:

- i. To calibrate DCP and DPL in a calibration chamber so that a correlation can be made between N_{10} and Relative Density for two different sizes of clean sand.
- ii. To develop a generalized correlation between P_{index} and Relative Density for clean sands of any particle size.
- iii. To verify the correlation in some dredge fill sites.

1.4 Methodology

The present study was carried out in three stages.

- (a) The air pluviation method was calibrated to know the height of fall and hole diameter of discharging bowl for a desired Relative Density of specific sand in the first stage.
- (b) In the second stage using this relation between Relative Density and height of fall, sand deposits of different relative densities were prepared in calibration chamber. On the prepared sand deposit DPL and DCP tests were performed. Penetration of cone was recorded for every blow of hammer. N_{10} and P_{index} value of DCP and DPL tests were determined. N_{10} is the number of blows per 10 cm of penetration of dynamic cone and P_{index} is the penetration rate of cone in mm/blow. To get a generalized correlation for various sizes of sand, P_{index}

values were normalized by multiplying it with $\sqrt{D_{50}}$. Then a generalized correlation between Relative Density and $P_{\text{index}}\sqrt{D_{50}}$ were found in DPL and DCP for clean sand of any particle size. It is noteworthy that DCP and DPL test data of Azad (2008) was also used to get the generalized correlation.

- (c) Finally the generalized correlation was verified from the test results in two dredge fill sites. At the same location Relative Density was determined using Sand Cone Method and dynamic cone resistance data. This data helped to improve the generalized correlation by incorporating depth correction factor (R_d) and fines correction factor (R_{FC}).

1.5 Organization of the Thesis

The thesis consists of five chapters and two appendices. In Chapter One, background and objectives of the research is described. Chapter Two contains the literature review where history, use and researches on DCP are described. In this chapter description of apparatus DCP and DPL are given. Chapter Three describes the testing arrangement and program. Chapter Four contains results and discussion. Chapter Five contains the conclusions and recommendations for further research. All graphs of DCP and DPL tests in calibration chamber are presented in Appendix A. Appendix B is the ASTM standard of DCP test.

CHAPTER 2 LITERATURE REVIEW

2.1 Introduction

The literature review given here is consisting of (a) principles of Dynamic Cone Penetrometer (DCP) test and Dynamic Probing, (b) description of DCP and Dynamic Probing Light (DPL) and (c) researches on DCP.

2.2 General Principle of Dynamic Probing

To drive a pointed probe (cone), a hammer of mass M and a height of fall H are used. Typical arrangement of Dynamic Probing is shown in Fig. 2.1. The hammer strikes on anvil which is rigidly attached to extension rods. The penetration resistance is defined as the number of blows required to drive the probe a defined distance. The energy of a blow is the mass of the hammer times the acceleration of gravity and times the height of the fall (MgH). Dynamic probing is mainly used in cohesionless soils. In interpreting the test results obtained in cohesive soils and in soils at great depth, caution has to be taken when friction along the extension rod is significant. Dynamic probing can be used to detect soft layers and to locate strong layers as, for example, in cohesion less soils for end bearing piles (DPH, DPSH). In connection with key borings, soil type and cobble and boulder contents can be evaluated under favorable conditions. After proper calibration, the results of dynamic probing can be used to get an indication of engineering properties, e.g. Relative Density, compressibility, shear strength, consistency etc. For the time being, quantitative interpretation of the results including predictions of bearing capacity remains restricted mainly to cohesionless soils; it has to be taken into account that the type of cohesionless soil (grain size distribution, etc.) may influence the test result.

2.3 Various types of Dynamic Probing

To indicate that a continuous record is obtained from the test in contrast to the expression probing is used, for example, the Standard Penetration Test (SPT). This is a simple test consisting of driving a rod with an oversize point at its base into the ground with a uniform hammer blow. Dynamic Probing (DP) is carried out as per BS 1377: 1990. The test involves driving a solid steel 90 degree cone into the bottom of the borehole. The blow count is recorded for every 10 cm of driving (N_{10}) and the results presented as a plot of blow count against depth. Four different probing types, DPL, DPM, DPH and DPSH are available to fit different topographic and geological conditions and various purposes of investigation. In Table 2.1 Differences among these four types of probing are summarized.

Dynamic Probing Light (DPL): Representing the lower end of the mass range of dynamic cone used world wide; the investigation depth usually is not larger than about 8 m if reliable results are to be obtained.

Dynamic Probing Medium (DPM): Representing the medium mass range; the investigation depth usually is not larger than about 20 to 25 m.

Dynamic Probing Heavy (DPH): Representing the medium to very heavy mass range; the investigation depth usually is not larger than about 25 m.

Dynamic Probing Super Heavy (DPSH): Representing the upper end of the mass range and simulating closely the dimensions of the SPT; the investigation depth can be larger than 25 m.

2.4 Specification of Dynamic Probing Light (DPL)

Dimensions and masses of DPL are given in Fig. 2.1 and Table 2.2. The driving device consists of the hammer, the anvil and the guide rod.

Anvil: Fig. 2.2 shows the anvil of DPL which is rigidly connected to the extension rod. The diameter of the anvil shall not be less than 100 mm and not more than the half the diameter of the hammer. The axis of the anvil, guide rod and extension rod shall be straight with a maximum deviation of 5 mm per meter. Total of mass of anvil and guide rod is 6 kg.

Hammer: The weight of hammer used here is 10 kg. The dimensions of the hammer are shown in Fig. 2.3. The hammer shall be provided with an axial hole with a diameter which is about 3-4 mm larger than the diameter of the guide rod. The ratio of the length to the diameter of the cylindrical hammer shall be between 1 and 2. The hammer shall fall freely and not be connected to any object which may influence the acceleration and deceleration of the hammer. The velocity shall be negligible when the hammer is released in its upper position.

Extension Rod: The extension rod material should have high toughness at low temperatures and high fatigue strength. It also should be of high-strength steel with high resistance to wear. Permanent deformation must be capable of being corrected. The rods shall be straight. Solid rods can be used; hollow rods should be preferred in order to reduce the weight of the rod. Joints shall be flush with the rods. The deflection (from a straight line through the ends) at the mid point of 1-m push rod shall not exceed 0.5 mm for the five lowest push rods and 1 mm for the remainder.

Cone: In Fig. 2.4, it shows a typical cone of DPL. The dimensions of cone are given in Table 2.2. The cone consists of a conical part (tip), a cylindrical extension, and a conical transition with a length equal to the diameter of the cone between the cylindrical extension and the rod. The cone, when new, shall have a tip with an apex angle of 90° . The tip of the cone may be cut (e.g. by wear) about less than 10% of the diameter from the theoretical tip of the cone. The maximum permissible wear of the cone is given in Table 2.2. The cone shall be attached to the rod in such a manner that it does not loosen during driving. Fixed or detachable cones can be used.

2.5 DCP

For the rapid in situ measurement of the structural properties of existing road pavements with unbound granular materials the Transportation Research Laboratory Dynamic Cone Penetration (TRL-DCP) test apparatus is designed. Continuous measurements can be made to a depth of 800 mm or to 1200 mm when an extension rod is fitted. The underlying principle of the DCP is that the rate of penetration of the cone, when driven by a standard force, is inversely related to the strength of the material as measured by the California Bearing Ratio (CBR) test where the pavement

layers have different strength, the boundaries between the layers can be identified and the thickness of the layers are determined.

Three operators are needed to operate the DCP; one to hold the instrument, one to raise and drop the weight and a technician to record the results. The instrument is held vertical; the weight is carefully raised up to the handle; then the weight is dropped on anvil freely. Care should be taken to ensure that the weight is touching the handle, but not lifting the instrument before it is allowed to drop. The operator lets the weight fall freely and does not lower it with his hand. If, during the test, the DCP tilts from the vertical, no attempt should be made to correct this as contact between the shaft and the sides of the hole will give rise to erroneous results. The test should be abandoned if the angle of the instrument becomes worse, causing the weight to slide on the hammer shaft and not fall freely,

A reading should be taken at increments of penetration of about 10 mm is recommended. However it is usually easier to take readings after a set numbers blows. It is therefore necessary to change the number of blows between readings according to the strength of the layer being penetrated.

2.5.1 History of DCP

The DCP, was developed in 1956 in South Africa as in situ pavement evaluation technique for evaluating pavement layer strength (Scala, 1956) which also known as the Scala penetrometer. Since then, this device has been extensively used in South Africa, the United Kingdom, the United States, Australia and many other countries, because of its portability, simplicity, cost effectiveness, and the ability to provide rapid measurement of in situ strength of pavement layers and subgrades. Recently DCP is standardized by ASTM (ASTM D 6951-03). The DCP has also been proven to be useful during pavement design and quality control program. The DCP, however, was not a widely accepted technique in the United States in the early 1980s (Ayers, 1990). De Beer (1991), Burnham and Johnson (1993), Tumay (1994); Newcomb et al (1994); Truebe and Evans (1995); Newcomb et al (1995); Parker et el (1998); and White et al (2002) have shown considerable interest in the use of the DCP for several

reasons. First, the DCP is adaptable to many types of evaluations. Second, there are no other available rapid evaluation techniques. Third, the DCP testing is economical.

2.5.2 Parts of DCP

The design specification of the parts has a tremendous impact on the results collected from the tests so various parts of the DCP are very important. The schematic diagram of DCP instrument is shown in Fig. 2.5. The instrument is made by Stainless Steel for better efficiency and longer life time. The various parts of DCP are described in the following paragraphs.

Probing Cone: The most important part of the DCP instruments is Probing cone. Probing cone enters through the sand as test starts. So the design of the probing cone must be perfect according to the standards. We use a probing cone of 1.95 cm high and the angle of the cone is 60° . The diameter of the probing cone at the edge is 2.25 cm. The cone size can affect the results significantly. The various dimensions of cone are shown in Fig. 2.6.

Anvil: Another important part of DCP is Anvil. The hammer falls on the anvil each time a data is intended to collect. The anvil is connected to the extension rod. It is also made of stainless steel. Anvil also contains the clamp which holds the scale in position shown in Fig. 2.7.

Guide Rod: Guide rod is used for guiding the hammer to fall on the anvil. It is made of stainless steel and the diameter of the guiding rod is 1.6 cm. The length of the guide rod without thread is 81.4 cm.

Hammer: In the DCP an 8 kg hammer is used. The hammer moves along the guide rod. The dimensions are given in Fig. 2.8.

Extension Rod: We can join extension rod one after another with each other and make a long rod for larger depth. Extension rods are 100 cm long and its diameter is 1.6 cm.

Handle: On the top of a guide rod a handle is attached. It helps the operator to hold the instrument in place and also a guide for the operator to move the hammer up to that level. The dimensions are shown in Fig. 2.9.

Damping Washer: Damping washer is put in the junction of hammer and the anvil. It lessens the collision sound and also extends the longevity of the instrument. It may be a piece of geo-textile or any damping material.

1 m Scale: For taking the reading of the penetrated rod in mm per blow a one meter stainless steel scale is also used.

2.5.3 Correlations with DCP

Researchers tried to establish correlation between other test parameters and DCP test results. In this section brief review of those correlations are presented.

Standard Penetration Test: Sowers and Hedges (1966), and later Livneh and Ishai (1988), developed a correlation between Penetration Index ($P_{\text{index, DCP}}$) and rate of penetration ($P_{\text{index, SPT}}$) in SPT sampler (ASTM D1586-64). By Penetration Index ($P_{\text{index, DCP}}$) they meant rate of penetration of DCP cone in mm/blow. They also expressed rate of penetration of SPT sampler ($P_{\text{index, SPT}}$) in mm/blow. Their correlation, which is valid for SPT < 0.40 inches/blow or 10 mm/ blow, is

$$\text{Log}_{10} (P_{\text{index, DCP}}) = -A + B \text{Log} (P_{\text{index, SPT}}) \text{-----} 2.1$$

Where,

$P_{\text{index, DCP}}$ = Penetration Index in mm/blow

$P_{\text{index, SPT}}$ = SPT sampler penetration rate in mm/blow

This correlation is shown in Fig. 2.10.

California Bearing Ratio (CBR): Many researches has been performed to develop empirical relationships between DCP penetration resistance and CBR (ASTM D4429-93) measurements (e.g., Kleyn, 1975; Harison, 1987; Livneh, 1987; Livneh and Ishai, 1988; Chua, 1988; Harison, 1983; Van Vuuren, 1969; Livneh, et. al., 1992; Livneh

and Livneh, 1994; Ese et. al., 1994; and Coonse, 1999). Based on the results of past studies, many of the relationships between DCP and CBR have the following form:

$$\text{Log}_{10}(\text{CBR}) = A - B \log_{10}(P_{\text{index, DCP}}) \text{-----} 2.2$$

Where A = constant that ranges from 2.44 to 2.60; and B = constant that ranges from 1.07 to 1.16. A summary of some of these correlations are presented in Table 2.3. Correlation found by Tom Burnham (1993) has been shown in Fig. 2.11. Tom Burnham (1993) concluded that DCP test can be an excellent substitute for the field CBR determination.

Unconfined Compressive Strength: McElvaney and Djatnika (1991), based on laboratory studies, have concluded that Penetration Index can be correlated to the Unconfined Compressive Strength (UCS) of soil-lime mixtures. The UCS is a measure of the cohesive strength of a soil. Correlation of Tom Burnham (1993) is shown in Fig. 2.11.

Elastic Modulus: Some researchers have developed correlation between Penetration Index and Elastic Modulus of soil. Chua (1988) presented a correlation and preliminary findings for several types of soil. De Beer et al (1991) examined this correlation and proposed equation in following form.

$$\text{Log}_{10}(E_{\text{eff}}) = A - B \text{Log}_{10}(P_{\text{index, DCP}}) \text{-----} 2.3$$

E_{eff} = Effective Elastic Moduli (MPa)

$P_{\text{index, DCP}}$ = Penetration Index (mm/blow)

Shear Strength of Cohesionless Granular Materials: Ayers et al (1989) carried out a laboratory study to determine relationships between Penetration Index and the shear strength properties of cohesionless granular materials. Prediction equations are of the form:

$$\text{DS} = A - B (P_{\text{index, DCP}}) \text{-----} 2.4$$

Where, DS = Deviator stress at failure for confining pressures of 5, 15, and 30 psi (35, 103, and 207 kPa).

The selection of the appropriate prediction equation requires an estimate of the confining pressure under field loading conditions, which was stated to require further investigation.

2.5.4 Application of Dynamic Cone Penetrometer (DCP)

Many countries use DCP for various purposes. It has various applications. The simplicity and the legibility of DCP have made it popular throughout the world. Some applications applied in the world are-

- i. Livneh (1987) showed that the layer thickness obtained from DCP tests correspond reasonably well to the thickness obtained from the test pits. It was concluded that the DCP test is a reliable alternative for project evaluation.
- ii. Tom Burnham (1993) reported that DCP can be used to determine weak spot in sub grade foundation of road. In October of 1991, DCP testing was done on a bridge embankment west of Sacred Heart, Minnesota, USA. At that site the contractor was having difficulty meeting embankment density requirements. Minnesota Road pavement research facility has been performed DCP test at that location. At the Minnesota Road pavement research facility DCP testing showed an extremely weak spot in the lower layers in one of the test section embankments. Penetration Indices were as high as an astounding 297 mm/blow at a depth of 762 mm while Penetration Index near the surface averaged less than 51 mm/blow (see Fig. 2.12). Additional tests in this area showed that the weak spot in that location.

Table 2.1: Technical data of the equipment used in Dynamic Probing

Factor	DPL	DPM	DPH	DPSH
Hammer mass, kg	10	30	50	63.5
Height of fall, m	0.5	0.5	0.5	0.75
Mass of anvil and guide rod (max), kg	6	18	18	30
Extension rod outer diameter, mm,	22	32	32	32
Extension rod inner diameter, mm	6	9	9	-
Cone diameter, mm	35.7	35.7	43.7	50.5
Apex angle, deg.	90	90	90	90
Cone taper angle, upper, deg.	11	11	11	11
Number of blows per cm penetration	10 cm; N ₁₀	10 cm; N ₁₀	10 cm; N ₁₀	20 cm; N ₂₀
Standard range of blows	3 – 50	3 – 50	3 – 50	5 – 100
Note : DPL = Dynamic Probing Light, DPM = Dynamic Probing Medium, DPH = Dynamic Probing Heavy, DPSH = Dynamic Probing Super Heavy.				

Table 2.2: Specification of Dynamic Probing Light

Factor	DPL
Hammer mass, kg	10 ± 0.1
Height of fall, m	0.5 ± 0.01
Mass of anvil and Guide rod (max), kg	6
Rebound(max),	50
Length of the diameter(D)	$\geq 1 \leq 2$
Ratio(hammer)	
Diameter of anvil(d), mm	$100 < d < 0.5d$
Rod length, m	1 ± 0.1
Maximum mass of rod, kg/m	3
Rod deviation(max), First 5m	1.0
Rod deviation(max), Below 5 m,	2.0
Rod eccentricity(max), mm	0.2
Rod OD, mm	22 ± 0.2
Rod ID, mm	6 ± 0.2
Apex angle, deg.	90
Nominal are of cone, cm^2	10
Cone diameter, new, mm	$35.7 \pm .3$
Cone diameter, (min), worn, mm	34
Mantle length of cone, mm	35.7 ± 1
Cone taper angle, Upper, deg.	11
Length of cone tip, mm	17.9 ± 0.1
Max wear of cone tip Length, mm	3
Number of blows Per cm penetration	$10 \text{ cm}, N_{10}$
Standard range of blows	3 - 50
Specific work per blow: $\text{Mgh/A}, \text{KJ/m}^2$	50

Table 2.3: Developed correlation of DCP with CBR (Amini, 2003)

Correlation Equation	Material tested	References
$\text{Log}(\text{CBR})=2.56-1.16\text{Log}(\text{P}_{\text{index,DCP}})$	Granular and cohesive	Livneh (1987)
$\text{Log}(\text{CBR})=2.55-1.14\text{Log}(\text{P}_{\text{index,DCP}})$	Granular and cohesive	Harison (1987)
$\text{Log}(\text{CBR})=2.45-1.12\text{Log}(\text{P}_{\text{index,DCP}})$	Granular and cohesive	Livneh et al (1992)
$\text{Log}(\text{CBR})=2.46-1.12\text{Log}(\text{P}_{\text{index,DCP}})$	Various soil type	Webster et al (1992)
$\text{Log}(\text{CBR})=2.62-1.27\text{Log}(\text{P}_{\text{index,DCP}})$	Unknown	Kleyn (1975)
$\text{Log}(\text{CBR})=2.44-1.07\text{Log}(\text{P}_{\text{index,DCP}})$	Aggregate base course	Ese et al (1995)
$\text{Log}(\text{CBR})=2.60-1.07\text{Log}(\text{P}_{\text{index,DCP}})$	Aggregate base course and cohesive	NCDOT (1998)
$\text{Log}(\text{CBR})=2.53-1.14\text{Log}(\text{P}_{\text{index,DCP}})$	Piedmont residual soil	Coonse (1999)

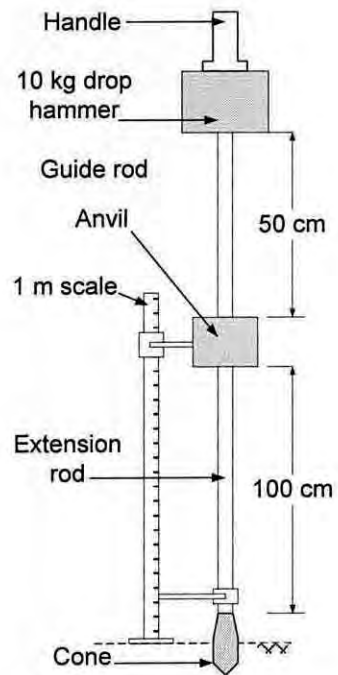


Fig. 2.1: Schematic diagram of Dynamic Probing Light (DPL)

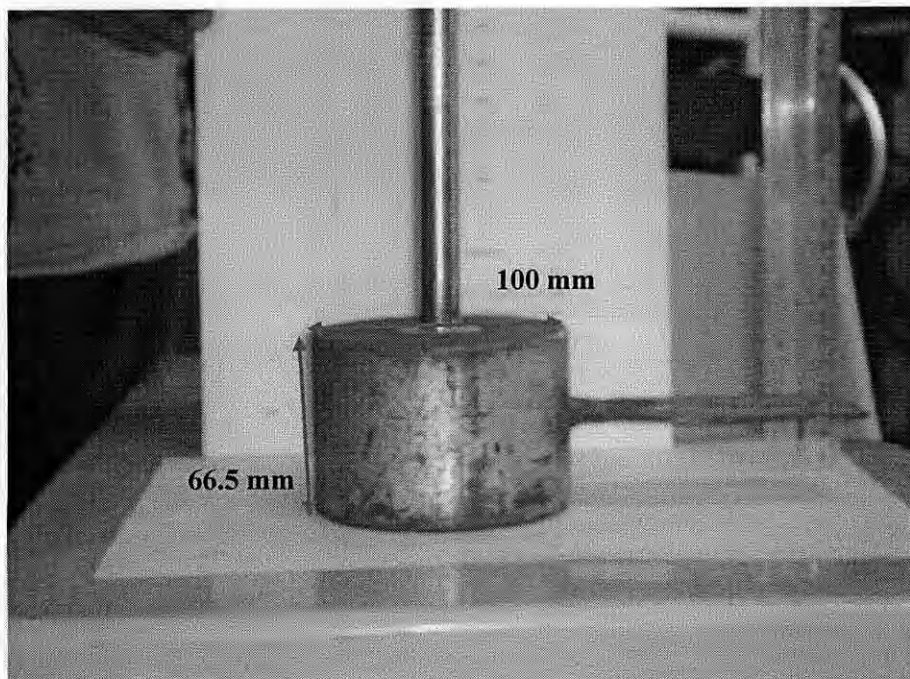


Fig. 2.2: The dimensions of 6 kg anvil of DPL

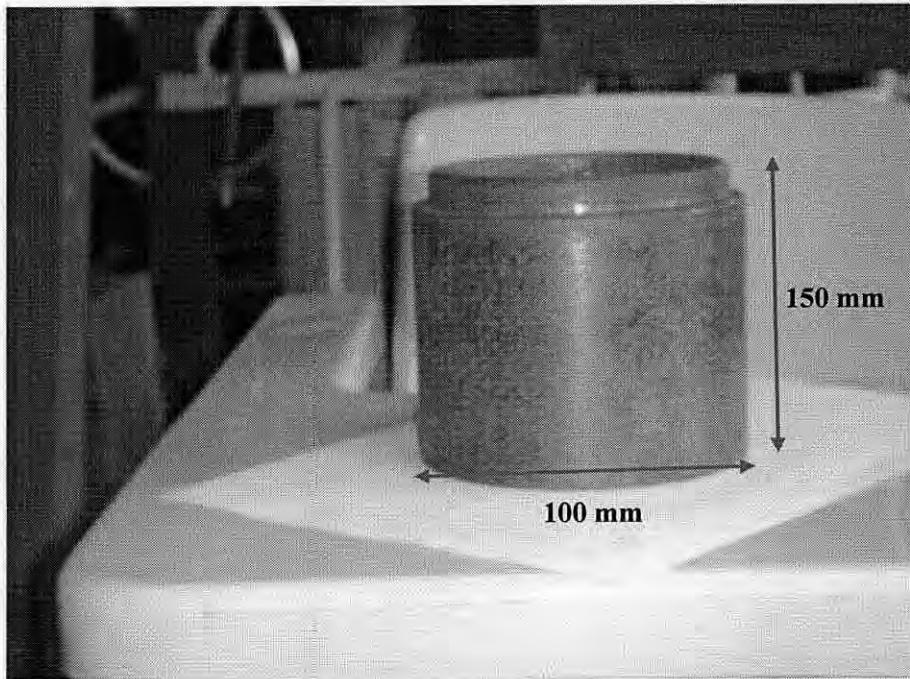


Fig. 2.3: Dimensions of 10 kg hammer of DPL

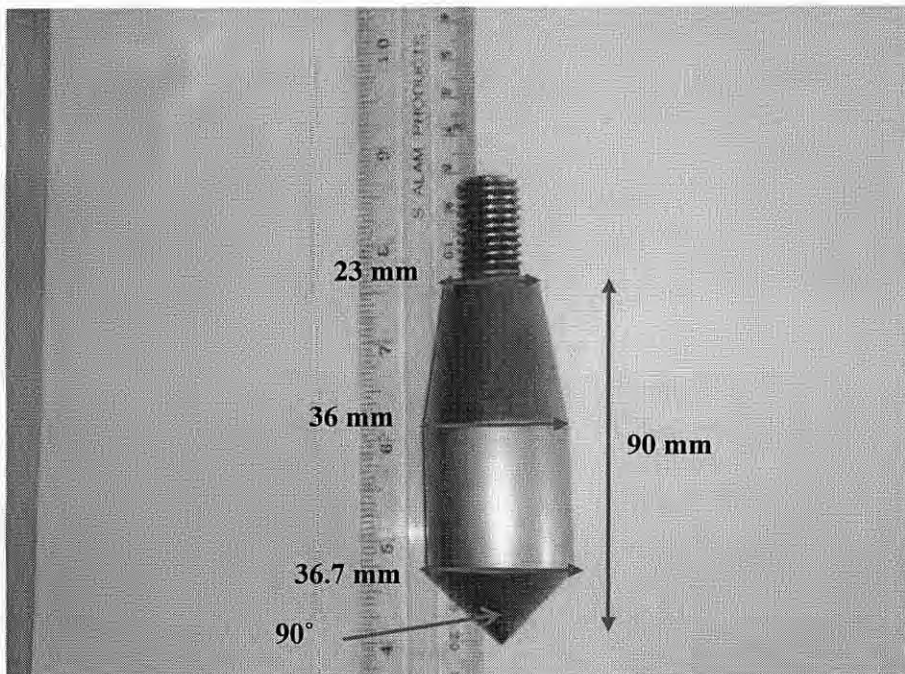


Fig. 2.4: Dimensions of Probing cone of DPL

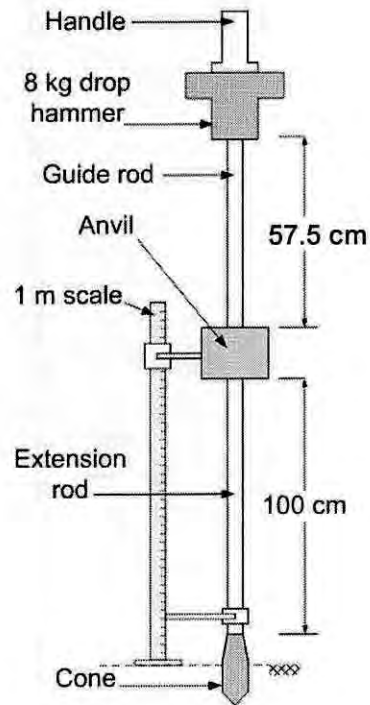


Fig. 2.5: Schematic diagram of Dynamic Cone Penetration (DCP) test

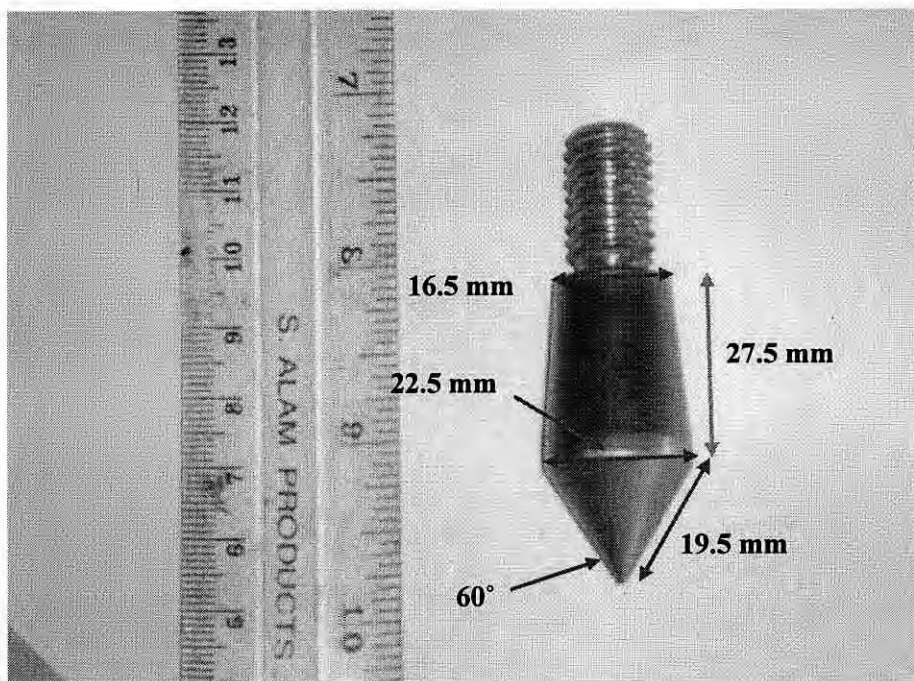


Fig. 2.6: Different dimensions of probing cone of DCP

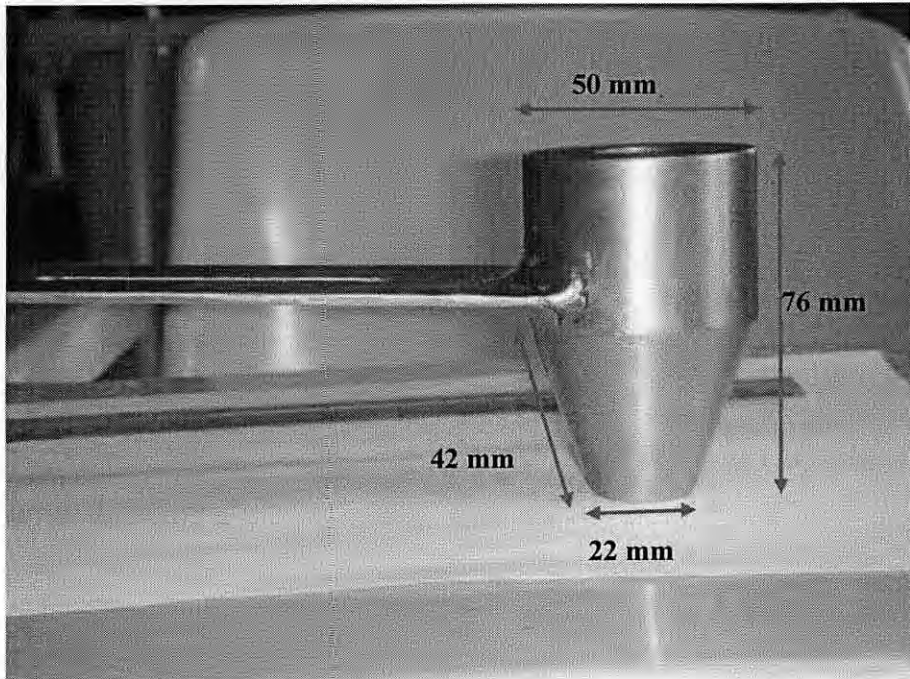


Fig. 2.7: Different dimensions of Anvil of DCP

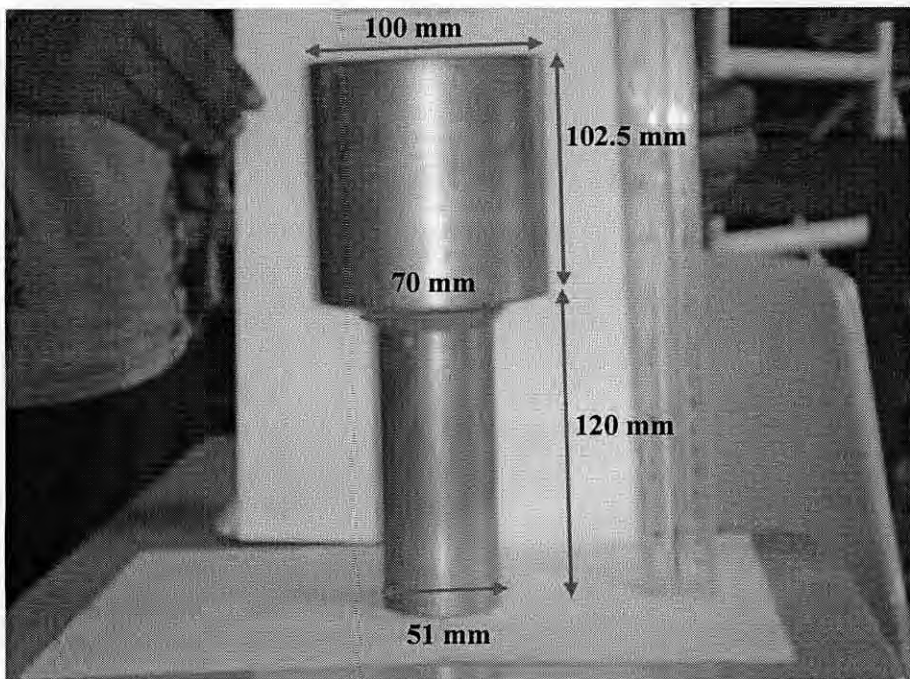


Fig. 2.8: Dimensions of 8 kg hammer of DCP

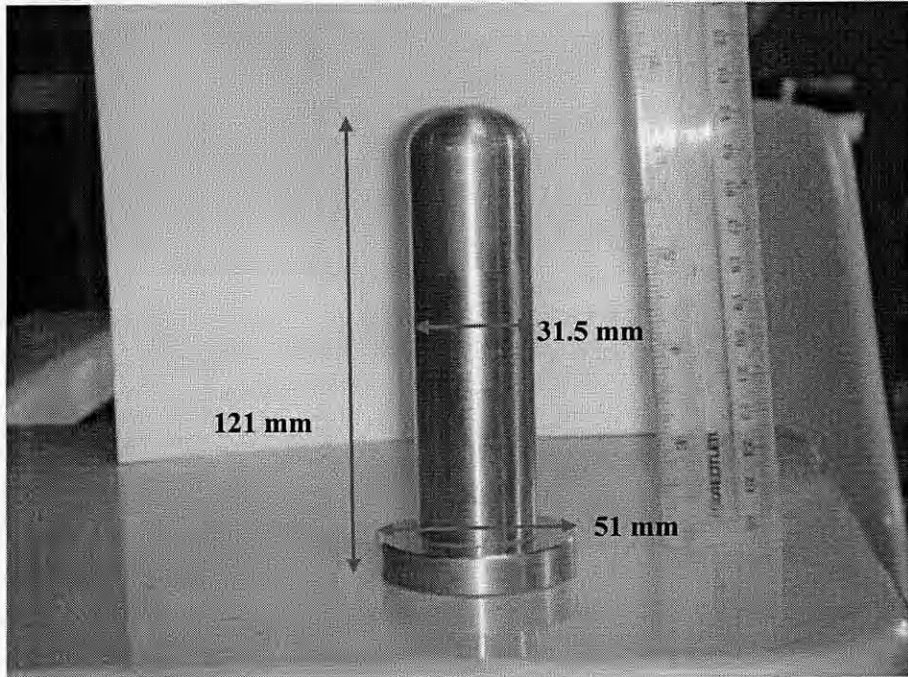


Fig. 2.9: Handle to hold DCP during test

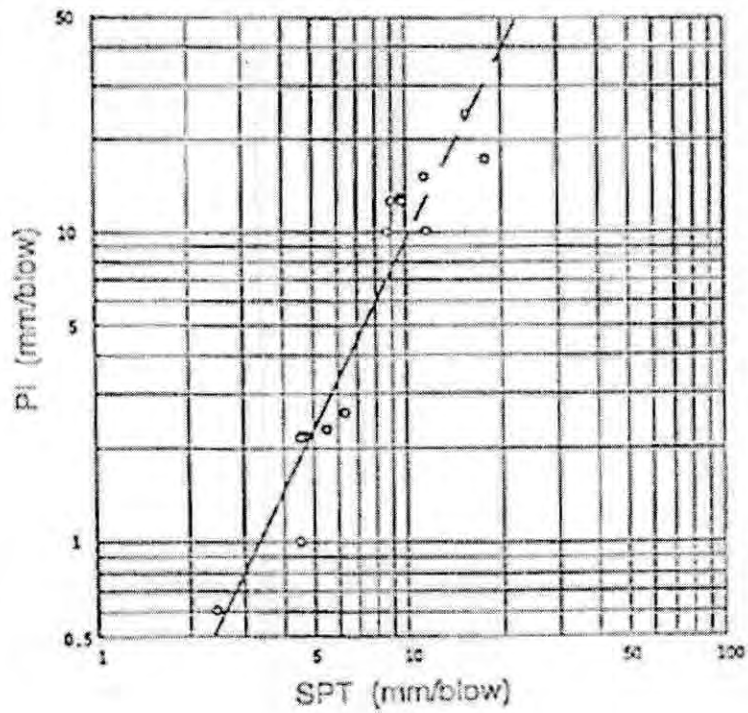


Fig. 2.10: Plot of Standard Penetration value vs Penetration Index (Tom Burnham, 1993)

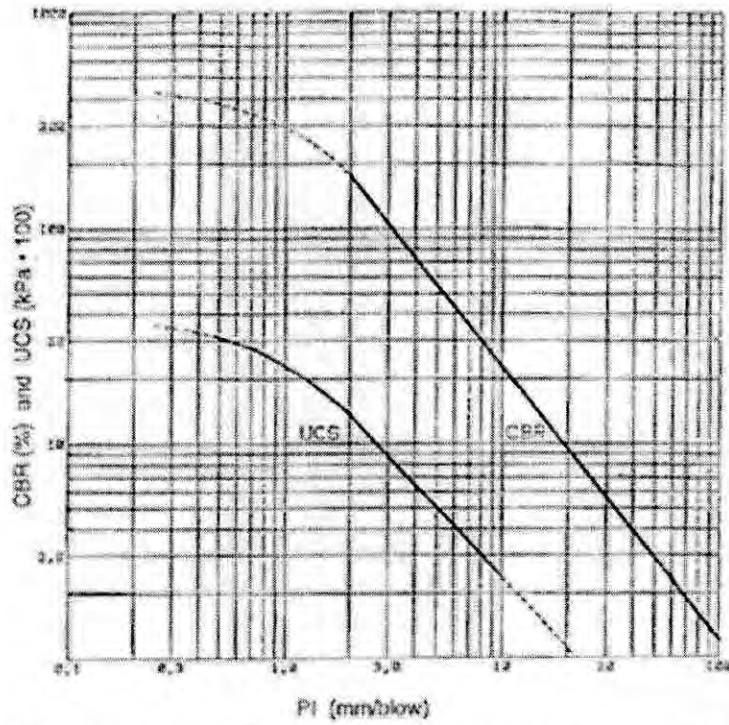


Fig. 2.11: Plot of California Bearing Ratio, Unconfined Compression Strength vs Penetration Index (Tom Burnham, 1993)

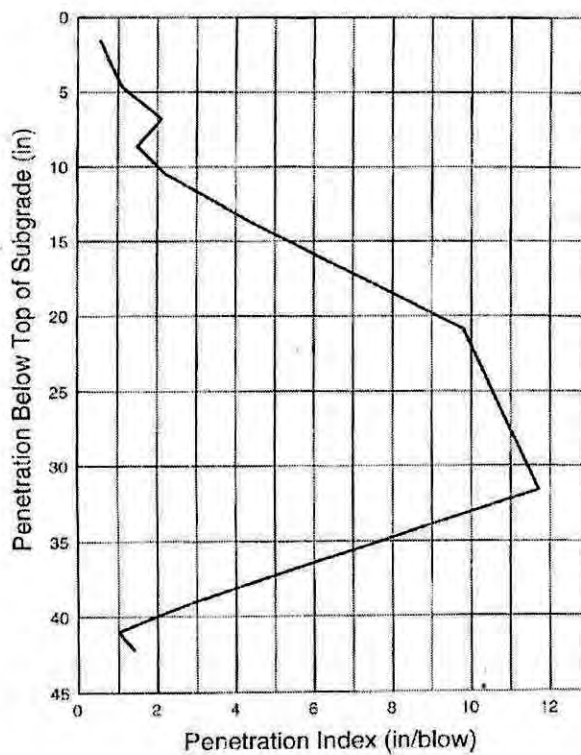


Fig. 2.12: The weak spot in subgrade bridge embankment. (Tom Burnham, 1993)

CHAPTER 3 TESTING PROGRAM

3.1 Introduction

The experimental program is described in this chapter. The experimental program consists of two stages. In the first stage, the air pluviation method was calibrated to know the height of fall and hole diameter of discharging bowl for different relative densities of two types of sand. In the second stage, sand deposits of different relative densities were prepared in calibration chamber where DPL and DCP tests were performed. Correlation between N_{10} and Relative Density was made from the test result in calibration chamber. Then correlation of P_{index} and Relative Density was made for any type of sand.

3.2 Calibration of Air Pluviation Method

By controlling height of fall & rate of sand discharge, sand of desired density can be prepared by Multiple Sieve Method and air pluviation method. Multiple sieving pluviation apparatus used by Miura and Toki (1982) is shown in Fig. 3.1. A simple air pluviation method was developed in the Geotechnical Laboratory to prepare sand deposit of desired density. A number of plastic bowls, shown in Fig. 3.2 has been used for this purpose. Holes of different diameters (3.5 mm, 4.0 mm and 5.0 mm) are punched into the plastic bowl. Hole to hole distance was 35 mm. A CBR mold was filled up by discharging sand from these holed bowls (hereafter called discharging bowl) maintaining fixed height of fall as shown in Fig 3.4. Then density of sand was determined by weighing sand in CBR mold. This procedure was repeated for different height fall to get different densities for a specific type of sand. Two types of sand were calibrated by this procedure; namely medium sand of FM 2.10 and fine sand of FM 1.33. Index properties of these sands are shown in Table 3.1. Grain size distributions of these two sands are shown in Fig. 3.5. Air pluviation calibration data are tabulated in Table 3.2 to 3.5.

3.3 DCP and DPL Tests in Calibration Chamber

To perform the DCP and DPL test a steel cylinder of diameter 0.5 m and height 1 m was used as a calibration chamber. The thickness of calibration chamber wall was 13 mm. Top and bottom of the cylinder was open.

3.3.1 Preparation of Sand Deposit in Calibration Chamber

The calibration chamber was placed on a level ground. For providing working platform for preparation and testing in chamber some bags filled with stone chips were placed around the chamber. To minimize disturbance of wind during sand deposition the chamber and working platform were surrounded by thick polythene sheets, as shown in Fig. 3.7,. Sands were air dried by spreading them on dry floor (shown in Fig. 3.8). Then sand deposit of desired density was prepared by air pluviation method described in section 3.2. Height of fall was maintained by suspending a small weight from the discharging bowl through a fixed length of rope. Dry deposition of sand is shown in Figs. 3.9 to 3.11. Sand deposit of various relative densities was prepared using this method.

To get higher Relative Density sand deposit was prepared by filling sand into chamber in 6 inches layers. Each layer was densified using concrete vibrator as shown in Fig. 3.12. Then DCP and DPL test was performed on the prepared sand deposit. The total weight of sand was measured to determine the density of sand deposit.

3.3.2 Tests in Calibration Chamber

The calibration chamber was filled up by discharging sand from the discharging bowls maintaining fixed height of fall. After filling the calibration chamber, every time DPL and DCP tests were performed and for each blow the penetration of cone was recorded. It is important to note that DCP and DPL has similar features except differences in cone size, weight of anvil, weight of drop hammer and height of fall. Table 3.6 shows the differences between DCP and DPL. In both cases, N_{10} is the number of blows required for 10 cm penetration of the cone. Fig 3.13 shows starting

of a DCP test after filling calibration. After completion of tests, sands were taken out from the calibration chamber and weighed by digital balance to check the density and Relative Density of sand deposit.

Table 3.1: Properties of two types of sands

Properties	Medium Sand	Fine Sand
Fineness Modulus	2.10	1.33
D_{10} (mm)	0.19	0.16
D_{30} (mm)	0.34	0.20
D_{50} (mm)	0.47	0.27
D_{60} (mm)	0.55	0.32
Uniformity Coefficient, C_u	2.89	2.00
Coefficient of Curvature, C_c	1.11	0.78
Maximum void ratio, e_{max}	1.23	1.21
Minimum void ratio, e_{min}	0.56	0.56
Maximum index density, γ_{max} (kN/m^3)	17.02	16.57
Minimum index density, γ_{min} (kN/m^3)	13.93	13.08
Fines (%)	0	0
Type (Unified Soil Classification)	SP (Clean Sand)	SP (Clean Sand)
Note : D_{10} (mm) = particle size corresponding to 10% finer, D_{50} (mm) = mean diameter of sand.		

Table 3.2: Calibration of air pluviation method for fine sand (Opening of discharging bowl 3.5 mm)

Relative Density vs Height of fall for fine sand			
Maximum dry density, $\gamma_{\max} = 16.57 \text{ kN/m}^3$		Minimum dry density $\gamma_{\min} = 13.08 \text{ kN/m}^3$	
Height of fall (cm)	Dry density, (kN/m ³)	Relative Density, Dr (%)	Opening of discharging bowl (mm)
15	14.13	35.23	3.5
30	14.84	56.21	3.5
45	15.51	74.36	3.5
60	15.59	76.53	3.5
75	15.76	80.66	3.5
90	15.85	83.08	3.5
105	15.93	84.97	3.5
120	15.97	85.86	3.5
135	16.00	86.58	3.5

Table 3.3: Calibration of air pluviation method for fine sand (Opening of discharging bowl 4.0 mm)

Relative Density vs Height of fall for fine sand			
Maximum dry density, $\gamma_{\max} = 16.57 \text{ kN/m}^3$		Minimum dry density $\gamma_{\min} = 13.08 \text{ kN/m}^3$	
Height of fall (cm)	Dry density, (kN/m ³)	Relative Density, Dr (%)	Opening of discharging bowl (mm)
15	13.74	22.65	4.0
30	14.49	46.26	4.0
45	15.31	69.18	4.0
60	15.61	76.85	4.0
75	15.74	80.14	4.0
90	15.82	82.23	4.0
105	15.90	84.20	4.0
120	15.96	85.63	4.0
135	15.99	86.34	4.0

Table 3.4: Calibration of air pluviation method for medium sand (Opening of discharging bowl 4.0 mm)

Relative Density vs Height of fall for medium sand			
Maximum dry density, $\gamma_{\max} = 17.02 \text{ kN/m}^3$		Minimum dry density $\gamma_{\min} = 13.93 \text{ kN/m}^3$	
Height of fall (cm)	Dry density, (kN/m ³)	Relative Density, Dr (%)	Opening of discharging bowl (mm)
15	15.58	58.47	4.0
30	16.05	72.82	4.0
45	16.14	75.52	4.0
60	16.21	77.36	4.0
75	16.28	79.55	4.0
90	16.31	80.41	4.0
105	16.32	80.73	4.0
120	16.33	81.00	4.0
135	16.39	82.58	4.0

Table 3.5: Calibration of air pluviation method for medium sand (Opening of discharging bowl 4.0 mm)

Relative Density vs Height of fall for medium sand			
Maximum dry density, $\gamma_{\max} = 17.02 \text{ kN/m}^3$		Minimum dry density $\gamma_{\min} = 13.93 \text{ kN/m}^3$	
Height of fall (cm)	Dry density, (kN/m ³)	Relative Density, Dr (%)	Opening of discharging bowl (mm)
15	14.74	30.13	5.0
30	15.45	54.11	5.0
45	15.82	65.89	5.0
60	15.93	69.05	5.0
75	16.04	72.44	5.0
90	16.14	75.54	5.0
105	16.23	78.18	5.0
120	16.30	80.01	5.0
135	16.31	80.19	5.0

Table 3.6: Basic differences between DCP and DPL

Parameters	DCP	DPL
Hammer (kg)	8	10
Height of fall (m)	0.66	0.50
Mass of anvil and guide rod (kg)	--	6
Cone diameter (mm)	22.5	35.7
Apex angle of cone (degree)	60	90

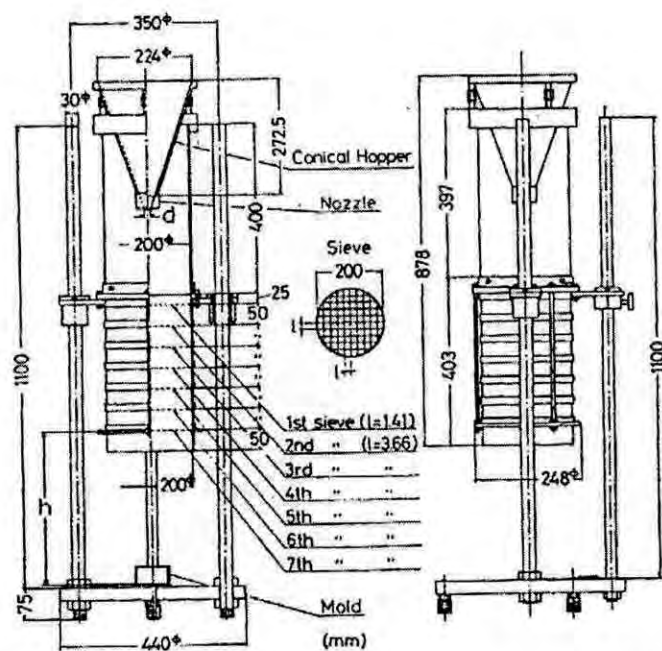


Fig. 3.1: General view of multiple sieving pluviation apparatus (Miura and Toki, 1982)

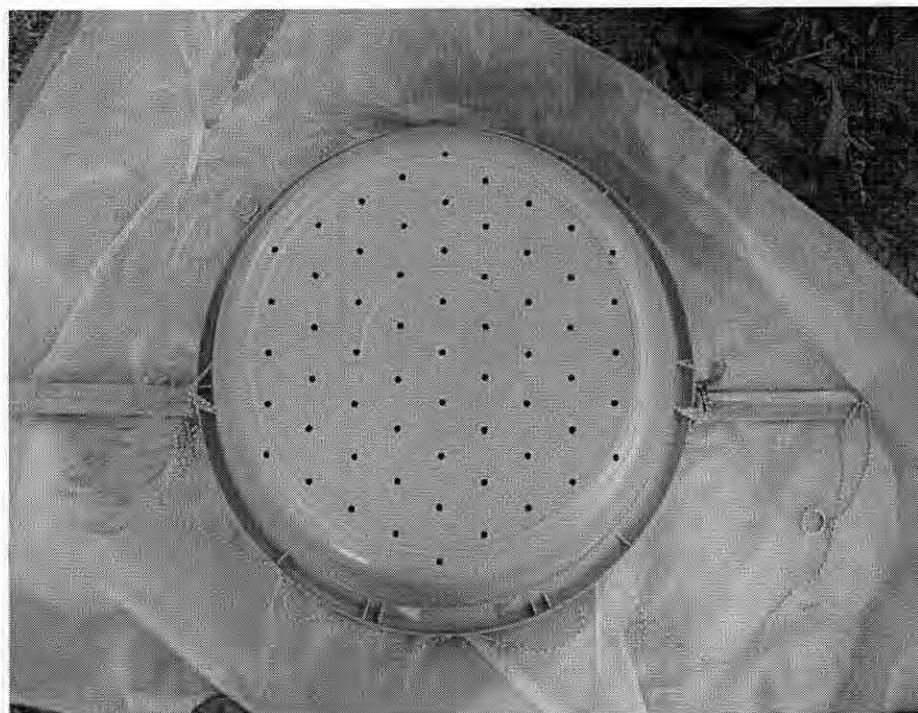


Fig. 3.2: Sand discharge bowl with 4 mm diameter holes

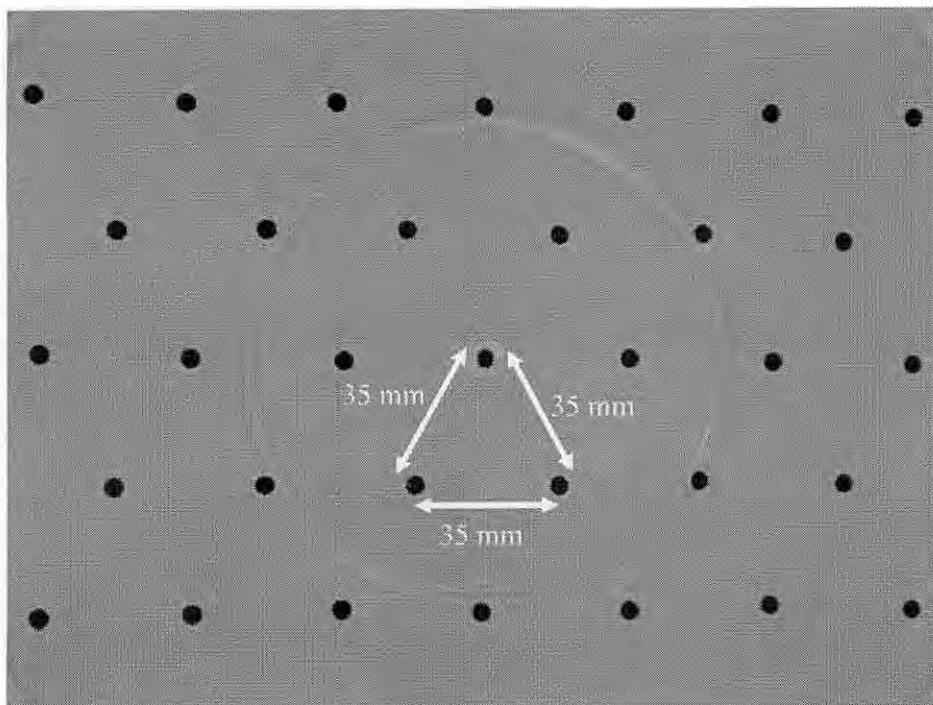


Fig. 3.3: Spacing and pattern of holes of discharge bowls.



Fig. 3.4: Air pluviation method

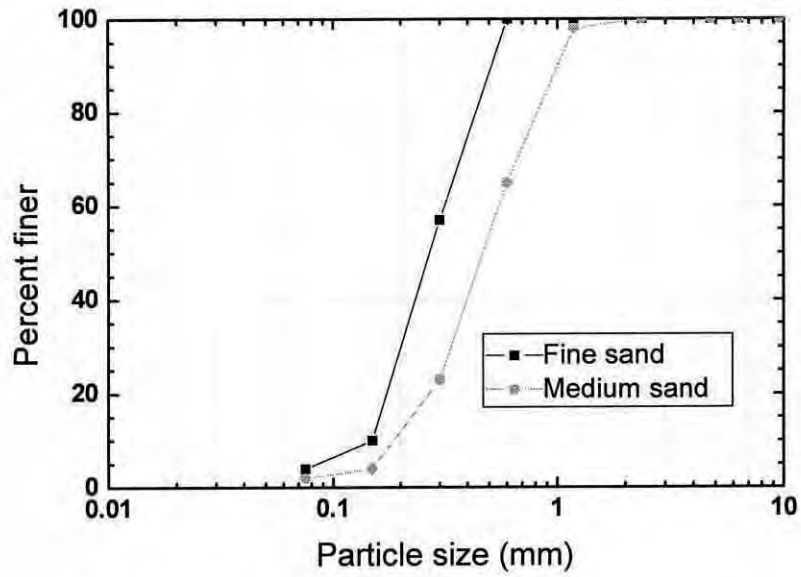


Fig. 3.5: Grain size distribution of fine sand and medium sand used in the study



Fig. 3.6: Calibration chamber and working platform



Fig. 3.7: Calibration chamber surrounded by thick polythene sheet to minimize disturbance by wind



Fig. 3.8: Drying of sand before test



Fig. 3.9: Dry deposition into calibration chamber from discharging bowl maintaining a constant height of fall

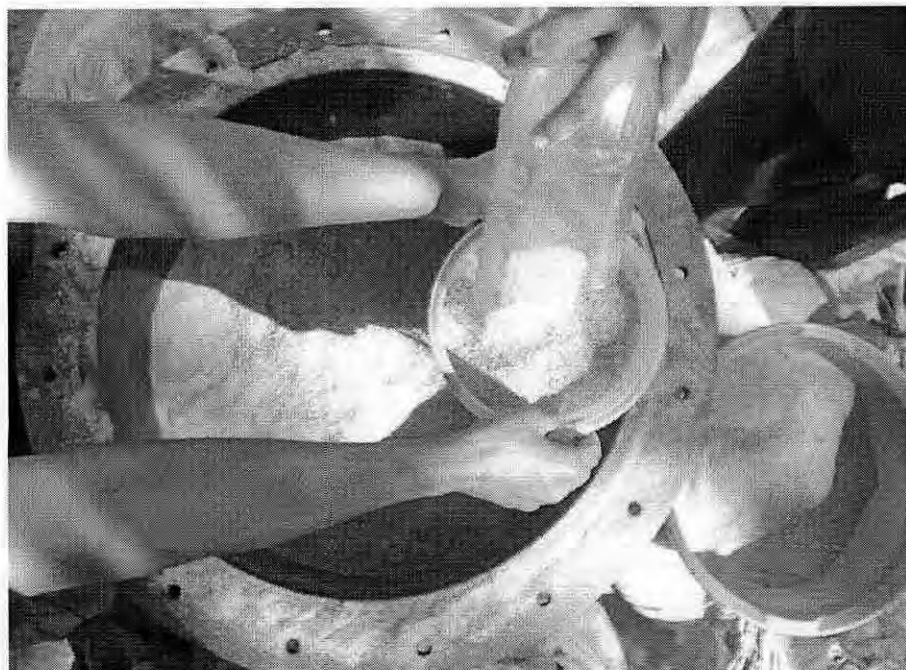


Fig. 3.10: Recharging of discharge bowl

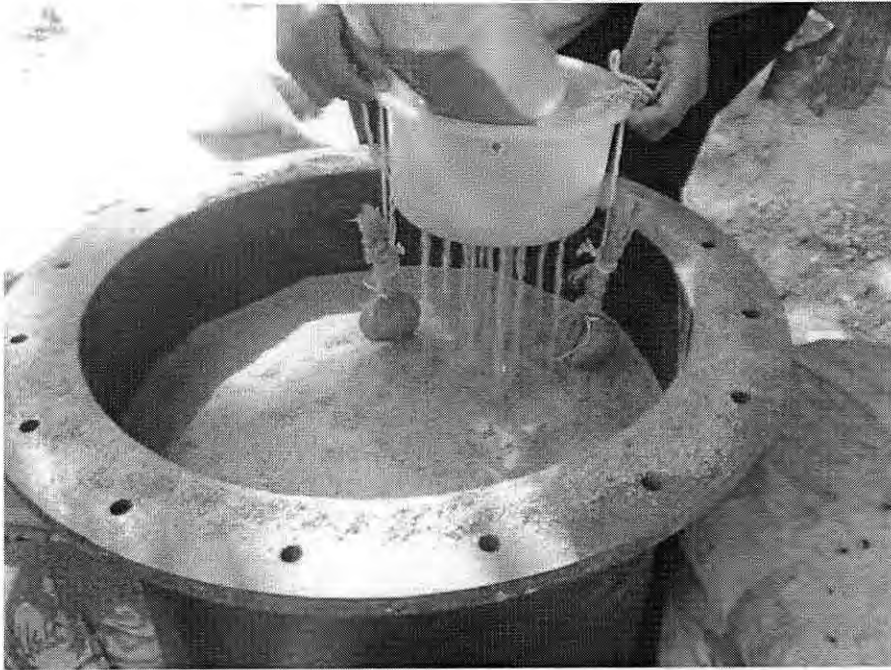


Fig. 3.11: Filling of calibration chamber in progress



Fig. 3.12: Densification of sand into calibration chamber using concrete vibrator



Fig. 3.13: Initial reading of the scale before starting DCP

CHAPTER 4 RESULTS AND DISCUSSION

4.1 Introduction

In this chapter the results of the experimental program are presented which include the calibration of air pluviation method for fine sand and medium sand and DCP and DPL test results in calibration chamber and field.

4.2 Calibration of Air Pluviation Method

The plot of Relative Density against height of fall for fine sand is presented in Fig 4.1. Discharge bowls with 3.5 mm and 4 mm opening were used for fine sand. Fig. 4.2 is the plot of Relative Density against height of fall for medium sand. Discharge bowls with 4 mm and 5 mm openings were used for medium sand. From Fig. 4.1 to 4.2 it is seen that for a certain diameter of hole of discharge bowl the Relative Density of sand increases with increase of height of fall. For a specific sand type and a fixed height of fall, Relative Density decreases with increase of opening size of discharge bowl (Fig. 4.1 and 4.2). That means if the rate of discharge of sand decreases, Relative Density increases for a constant height of fall. To prepare sand deposit of known Relative Density, Fig. 4.1 to 4.2 were used to find the height of fall required for that Relative Density.

4.3 Result of DCP and DPL in Calibration Chamber

Sand deposit of uniform density was prepared in calibration chamber and then one DCP and one DPL test was performed on prepared sand deposit. Determination of P_{index} , N_{10} , Relative Density and correlation between P_{index} and Relative Density of medium sand and fine sand are presented in the following sections.

4.3.1 Determination of P_{index} and N_{10}

Sand deposit of desired Relative Density was prepared in calibration chamber, then one DCP and one DPL tests were performed in the chamber. Then recorded cumulative numbers of blows were plotted against depth. Fig. 4.3 and 4.4 show such plots for fine sand of Relative Density 67.97%. Some unreliable data points up to depth of 30 cm were eliminated because of presence of very low confining pressure on top of sand deposit. It is observed that cumulative number of blows increases linearly with depth after this elimination. Fig. 4.3 and 4.4 indicates uniform density of sand from top to bottom of sand deposit. P_{index} was calculated from the average slope of the cumulative number of blow vs depth plot, as shown in Fig. 4.3. Then N_{10} value was calculated as $100/P_{index}$. In Fig. 4.5 and 4.6 shows typical DCP and DPL test results for medium sand.

It was difficult to obtain Relative Density more than 72% by air pluviation method so by using concrete vibrator we prepare sand deposit of Relative Density 90.21%. DCP and DPL test result on fine sand of Relative Density 90.21% are shown in Fig. 4.7 and 4.8. From these figures it was seen that sand deposit was almost uniform throughout the depth. All other test results of DCP and DPL are presented in Appendix A.

4.3.2 Development of Correlation between Relative Density and P_{index}

To calculate the density of sand in calibration chamber all the sands were removed from the chamber and weighed after completion of DCP and DPL on prepared sand deposit. Then the Relative Density was calculated from the density. Following the procedure described in the previous section, P_{index} and N_{10} value for DCP and DPL was determined. To get a generalized correlation, P_{index} value is multiplied by $\sqrt{D_{50}}$ of sand where D_{50} is in mm. Then Relative Density vs $P_{index}\sqrt{D_{50}}$ is plotted in Fig. 4.9 and Fig. 4.10. Generalized correlation for DCP is expressed as

$$D_r(\%) = 97.4035.e^{\frac{-P_{index}\sqrt{D_{50}}}{80.7707}} + 3.0971 \text{-----} 4.1$$

Generalized correlation for DPL is expressed as

$$D_r(\%) = 104.3312.e^{\frac{-P_{\text{index}}\sqrt{D_{50}}}{18.1307}} - 1.4769 \text{-----} 4.2$$

Where,

D_r = Relative Density (%),

P_{index} = Penetration Index (mm/blow)

D_{50} = Mean diameter of sand particles in mm

Normalization of P_{index} by multiplying $\sqrt{D_{50}}$ was found to be appropriate to make generalized correlation for clean sands of any particle size.

4.4 Verification of Correlation from Field Data

After establishing generalized correlation between Relative Density and P_{index} from the test results in calibration chamber, the correlation was verified by the field test data of Jamuna Site and Pangaon site performed by Azad (2008). Fig. 4.11 shows a typical plot of number of blows vs depth of DPL test in Pangaon Site. This type of plot is useful to identify the layers of sand deposit. In the graph shown here clearly identified three distinct layers of sand. Uniform slope indicates a distinct layer. Slope changes where at the interface of the two layers. Penetration Index at any depth was calculated as an average penetration rate (mm/blow) of cone in five blows around that depth. A typical plot of depth vs Penetration Index is shown in Fig. 4.12. Using generalized correlation mentioned in Equation 4.1 and 4.2, Relative Density was calculated from Penetration Index which is shown in Fig. 4.13.

Field dry density at various depths of the same location where DCP and DPL test was performed was determined using Sand Cone Method. After determination of maximum and minimum index density of that sand, Relative Density was calculated from the field dry density obtained from Sand Cone Method. Relative Density thus obtained from DCP and DPL at various locations was compared with that obtained

from Sand Cone Method which is shown in Fig. 4.14. It shows that DCP and DPL give less Relative Density than Sand Cone Method. Two reasons were assumed to be the cause of these differences between results from DCP-DPL and Sand Cone Method. One is the depth and another is fines content. At shallow depth and ground surface, DPL and DCP encounter less resistance of penetration due to zero to very low confining pressure. On the other hand, during calibration of DCP and DPL in calibration chamber the sand was clean sand. In field fines content is about 5% which increases the density of the deposit without increasing cone resistance. Therefore two correction factors were introduced in Equation 4.1 and 4.2, one is correction factor for depth (R_d) and another is correction factor for fines content (R_{FC}). Generalized equation for DCP can expressed as

$$D_r(\%) = \left(97.4035.e^{\frac{-P_{index}\sqrt{D_{30}}}{80.7707}} + 3.0971 \right) R_d R_{FC} \text{-----4.3}$$

Generalized equation for DPL can be expressed as

$$D_r(\%) = \left(104.3312.e^{\frac{-P_{index}\sqrt{D_{30}}}{18.1307}} - 1.4769 \right) R_d R_{FC} \text{-----4.4}$$

Where,

$$R_d = \left(\frac{0.8}{d} \right)^{0.03} \text{-----4.5}$$

$$R_{FC} = 1 + 0.003F_c \text{-----4.6}$$

R_d = Correction factor for depth

R_{FC} = Correction factor for fines content

d = depth (m)

F_c = Fines content (%)

Equations 4.1 and 4.2 are valid for clean sand having no fines content. Equation 4.3 and 4.4 are valid for sand having fines content 0 to 15%. Equations 4.5 and 4.6 for correction factors are established using trial and error method. These two equations should be modified based on more experimental results in sand having fines content.

Using equations 4.3 and 4.4, Relative Density at various locations and depth were determined from Penetration Index of DCP and DPL and compared with Relative Density from Sand Cone Method in Fig. 4.15 and 4.16. It is clear that Relative Density from DCP and DPL are in good agreement with the Relative Density from Sand Cone Method. Relative Density at various locations determined from DCP, DPL and Sand Cone Method are plotted against depth and shown in Fig. 4.17 to 4.20. It is proved that instead of Sand Cone Method, DCP and DPL can be successfully used to determine Relative Density of sand deposit.

4.5 Findings

The following are the findings discussed in the previous sections:

- i. A generalized correlation between Relative Density and $P_{\text{index}}\sqrt{(D_{50})}$ was established for sizes of sand having fines content less than 15%, which was successfully applied in two dredge fill sites.
- ii. The larger the particle size greater be the resistance to penetration for a certain Relative Density of sand. Denser sand gives more resistance for a specific type of sand. Resistance of sand increases exponentially with Relative Density.
- iii. Air pluviation method can produce sand deposit of uniform and known Relative Density.

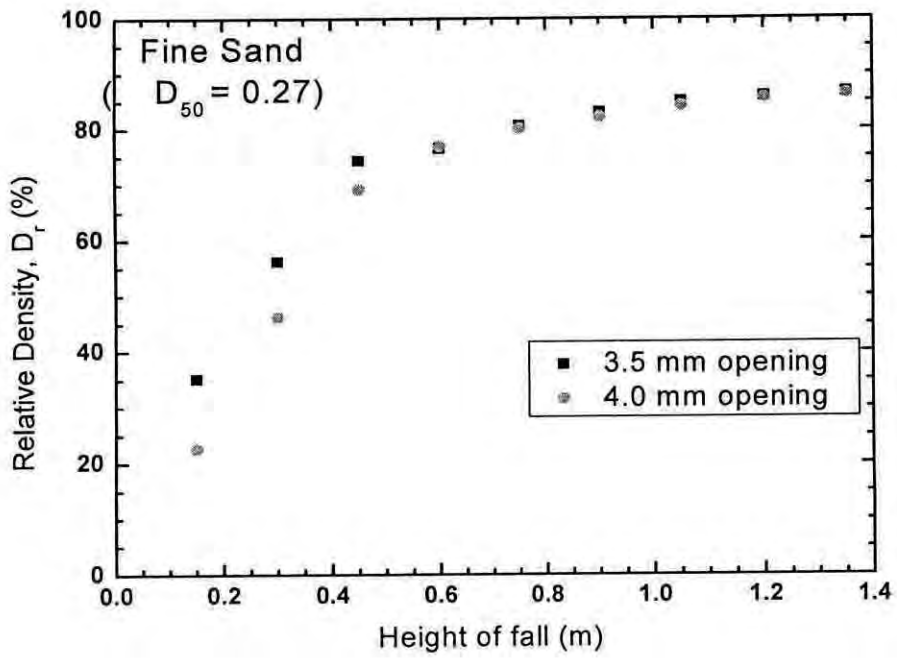


Fig. 4.1: Relative Density vs height of fall for fine sand

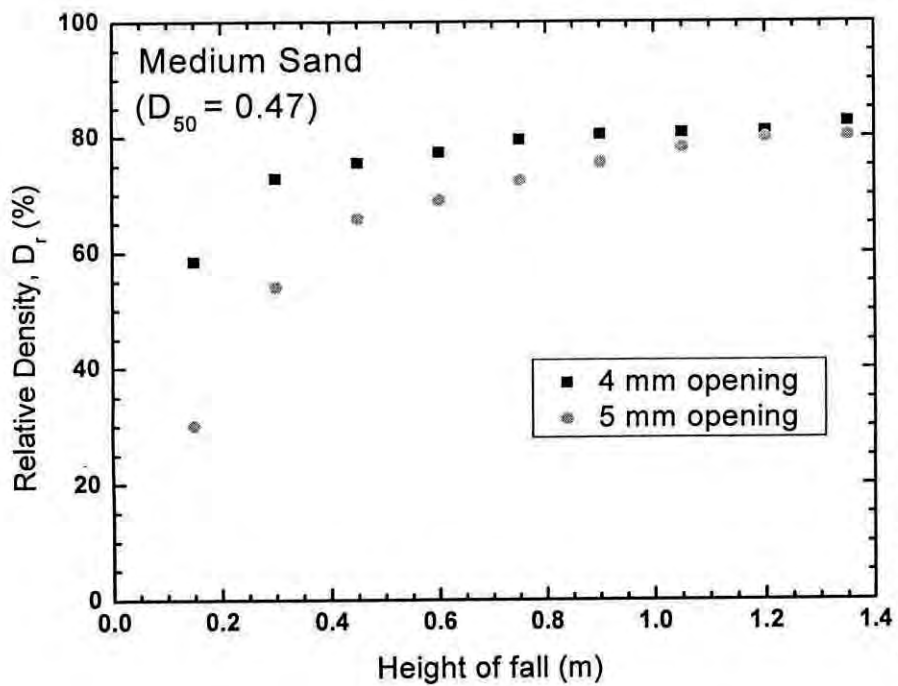


Fig. 4.2: Relative Density vs height of fall for medium sand

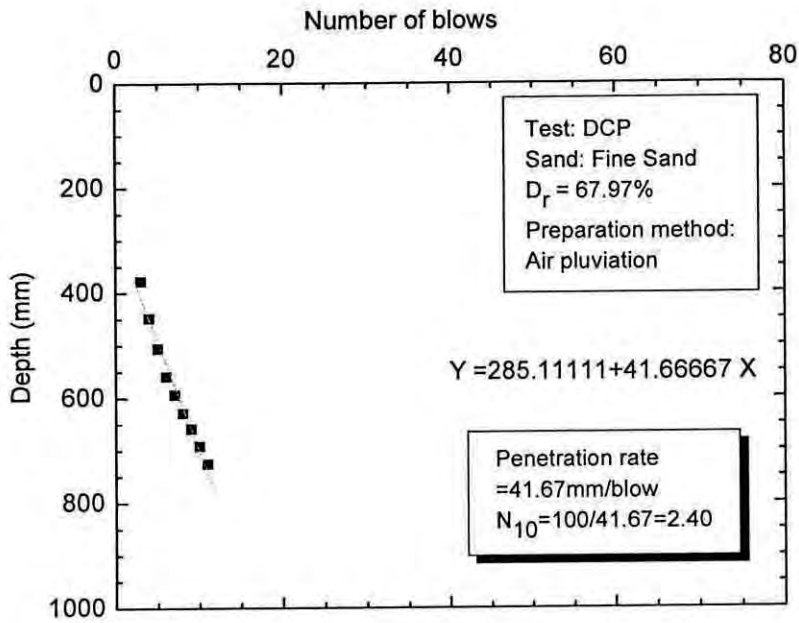


Fig. 4.3: Typical plot of number of blows vs depth (DCP) plot for fine sand in calibration chamber

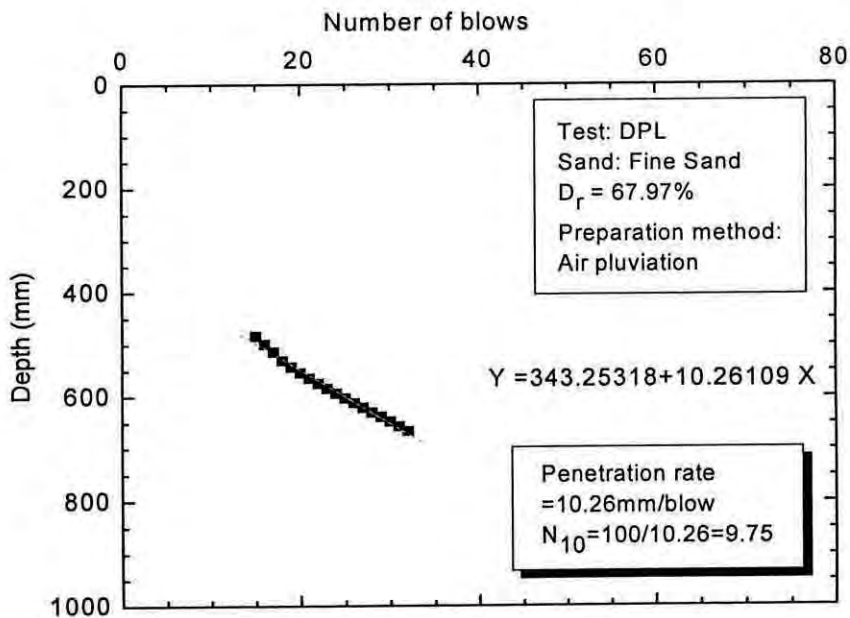


Fig. 4.4: Typical plot of number of blows vs depth (DPL) plot for fine sand in calibration chamber

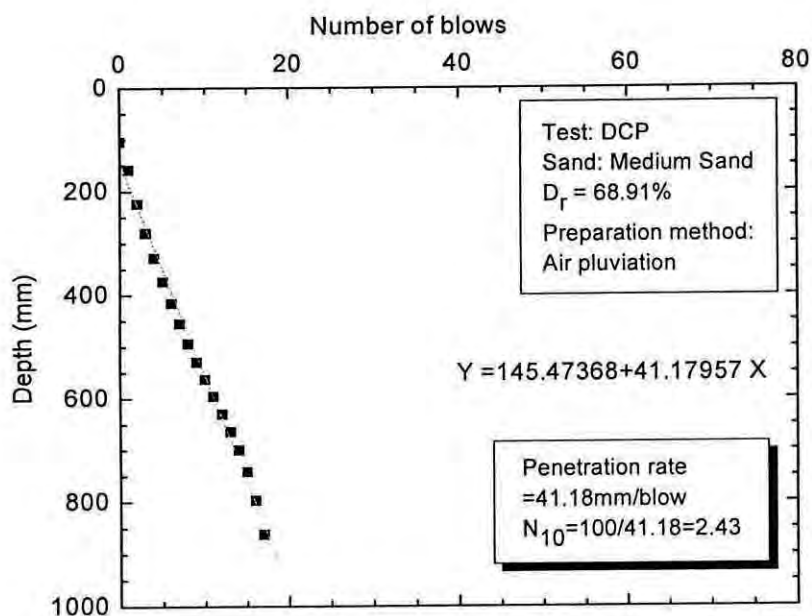


Fig. 4.5: Typical plot of number of blows vs depth (DCP) for medium sand in calibration chamber

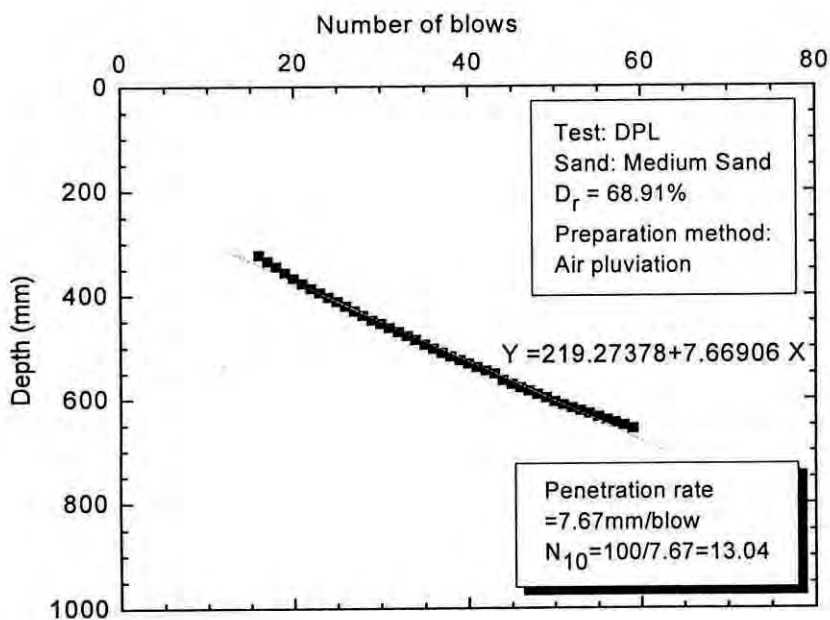


Fig. 4.6: Typical plot of number of blows vs depth (DPL) for medium sand in calibration chamber

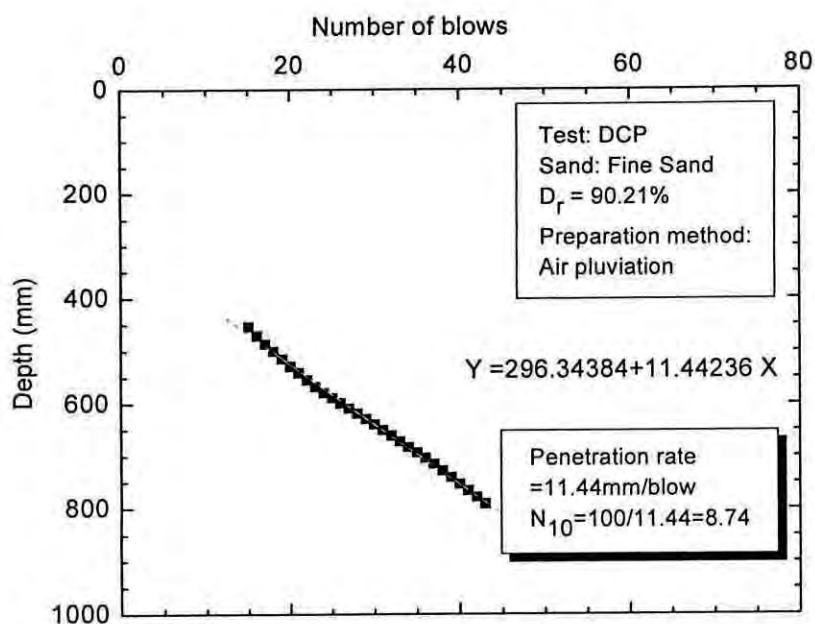


Fig. 4.7: Typical plot of number of blows vs depth (DCP) for fine sand in calibration chamber (Vibration method)

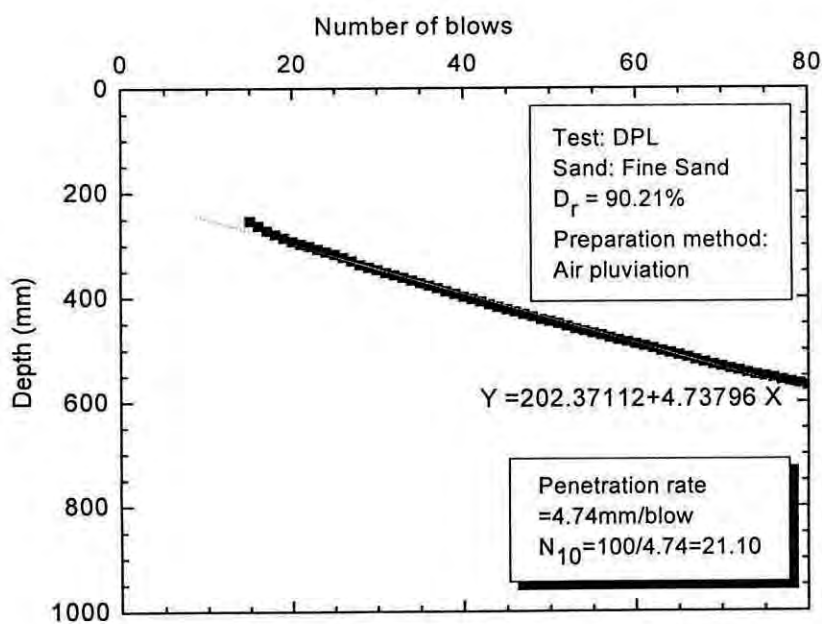


Fig. 4.8: Typical plot of number of blows vs depth (DPL) for fine sand in calibration chamber (Vibration method)

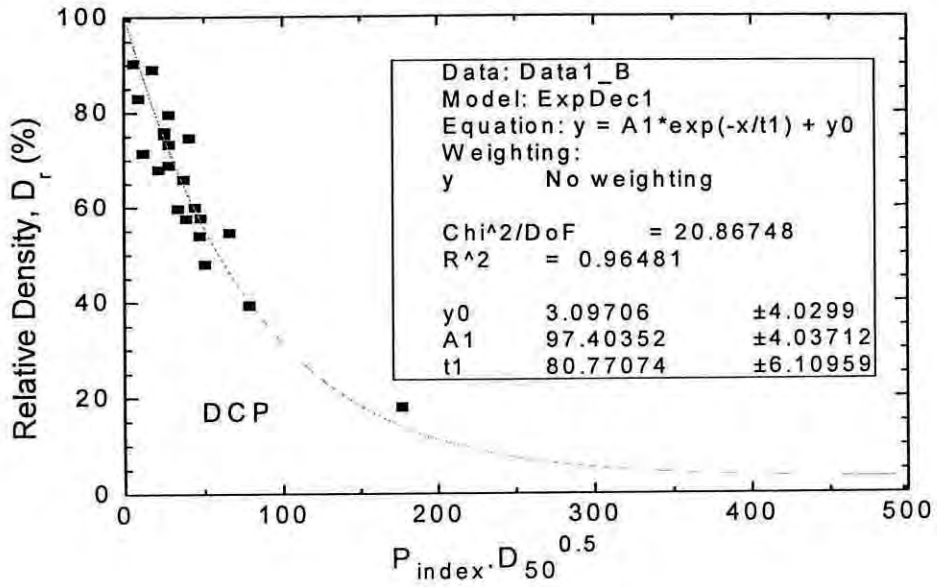


Fig. 4.9: Correlation between Relative Density and $P_{index} \times \sqrt{(D_{50})}$ of DCP for any sand (Linear scale)

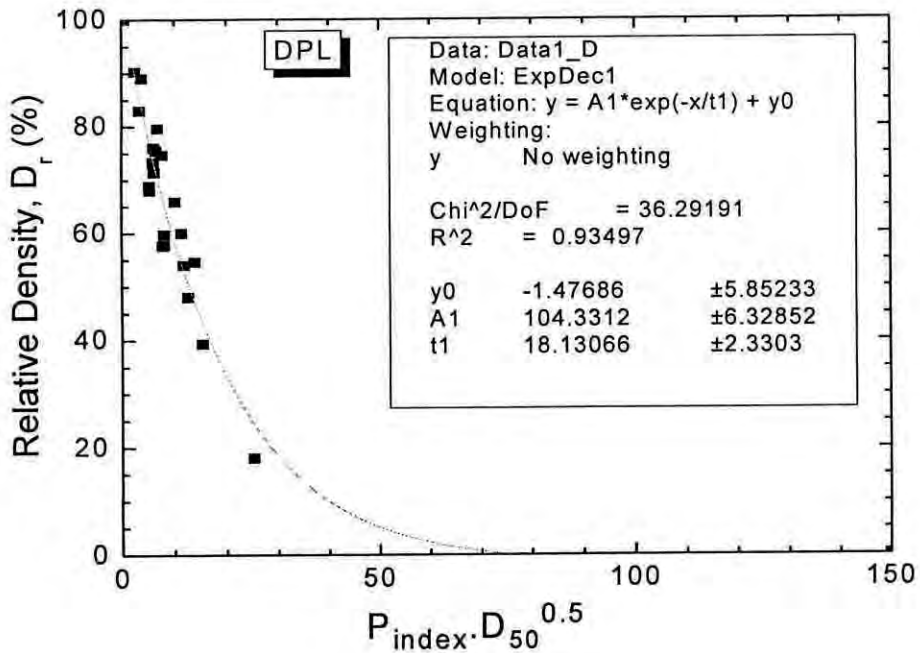


Fig. 4.10: Correlation between Relative Density and $P_{index} \times \sqrt{(D_{50})}$ in DPL for any sand (Linear scale)

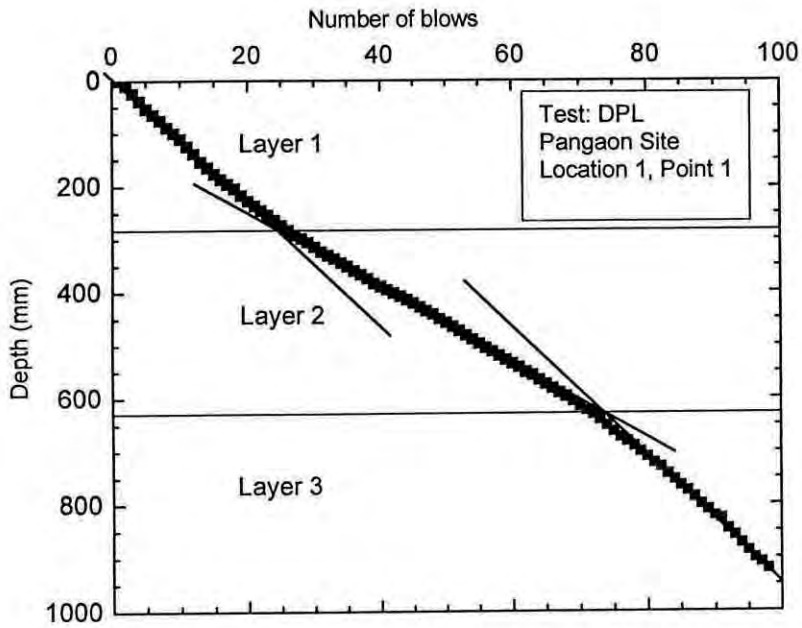


Fig. 4.11: Typical plot of number of blows vs depth of DPL test in Pangaon Site

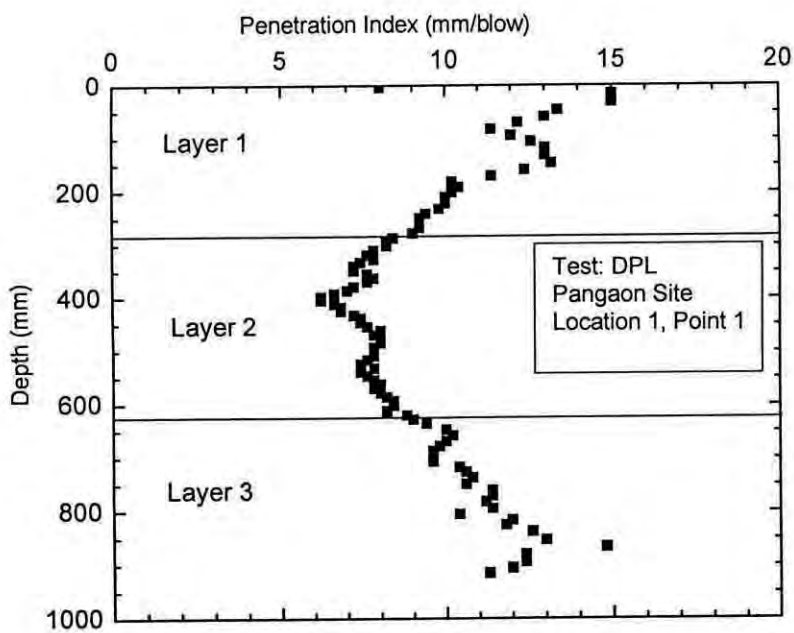


Fig. 4.12: Typical plot of Penetration Index vs depth of DPL test in Pangaon Site

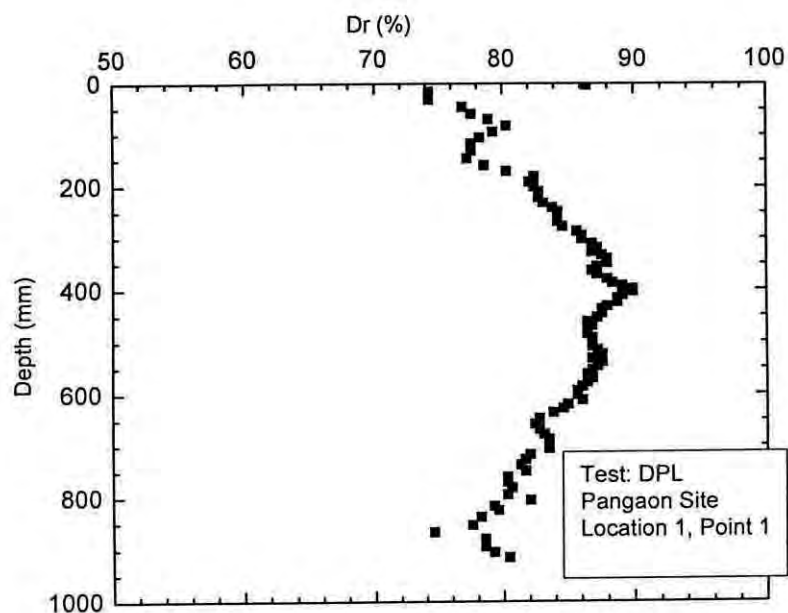


Fig. 4.13: Typical plot of Relative Density vs depth obtained from DPL test in Pangaon Site

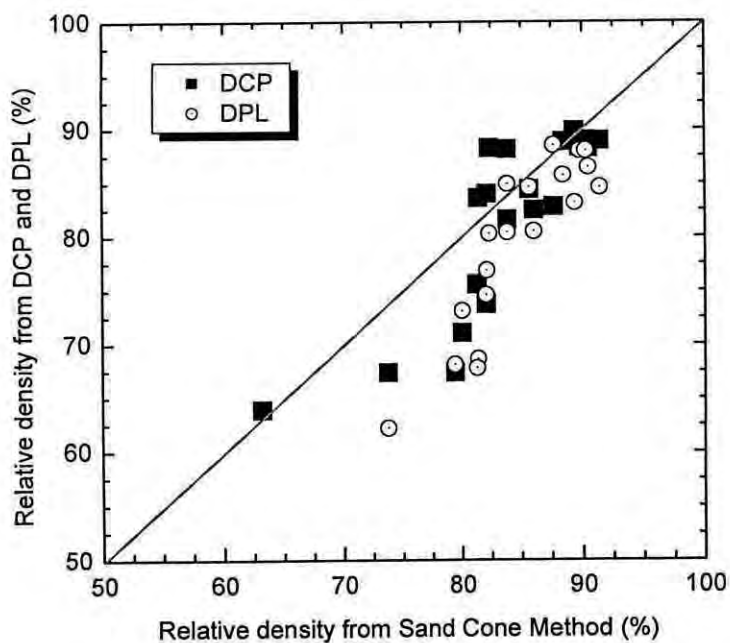


Fig. 4.14: Comparison of Relative Density obtained from DCP and DPL test and Sand Cone Method before introduction of correction factor

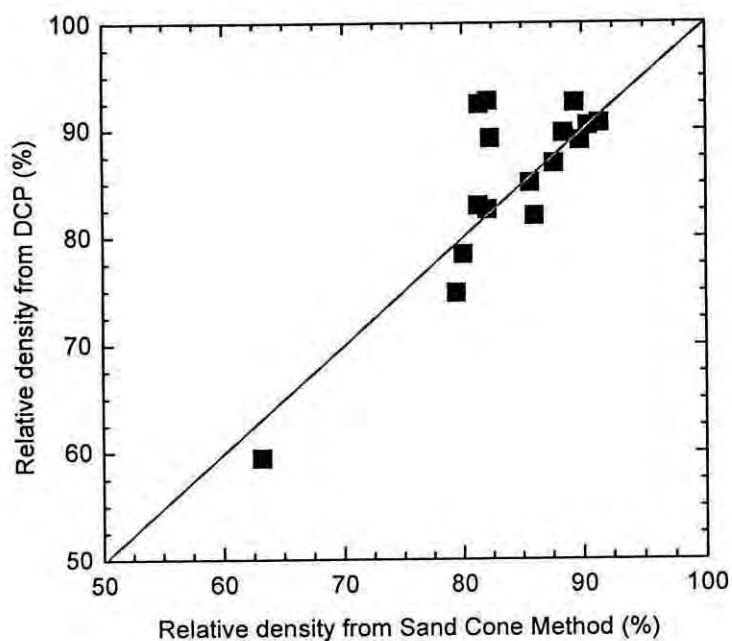


Fig. 4.15: Comparison of Relative Density obtained from DCP test and Sand Cone Method after introduction of correction factor

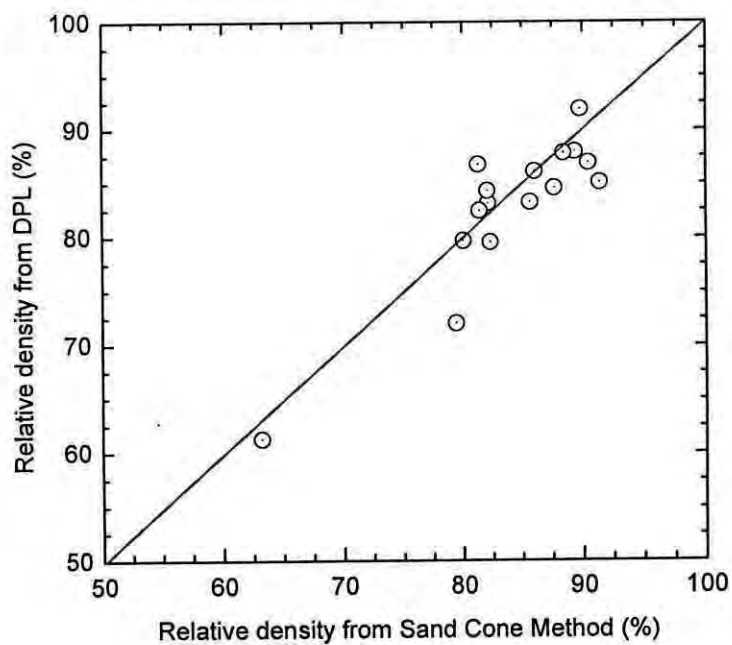


Fig. 4.16: Comparison of Relative Density obtained from DPL test and Sand Cone Method after introduction of correction factor

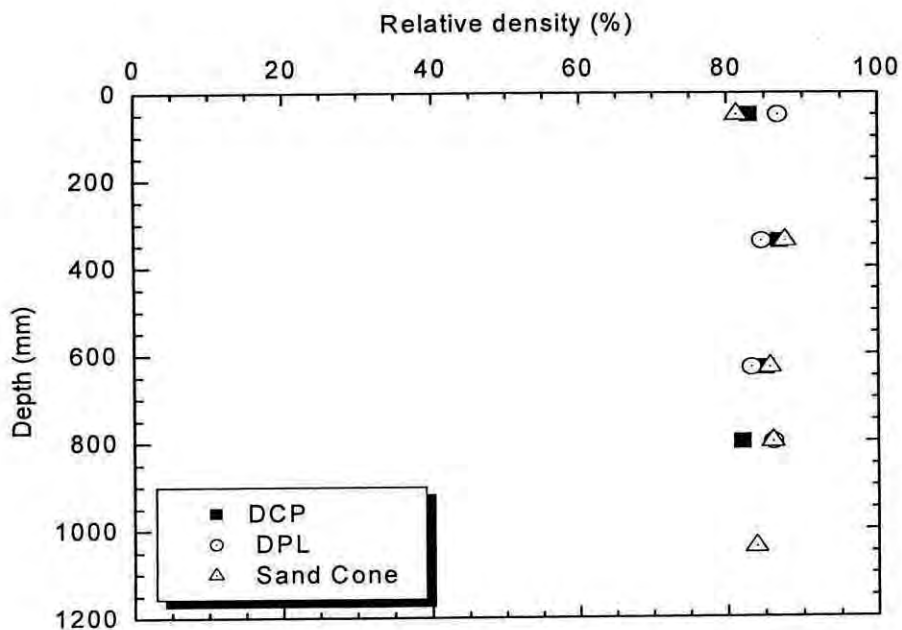


Fig. 4.17: Relative Density vs depth obtained from DCP, DPL and Sand Cone Method (Location 1, Point 1, Jamuna site)

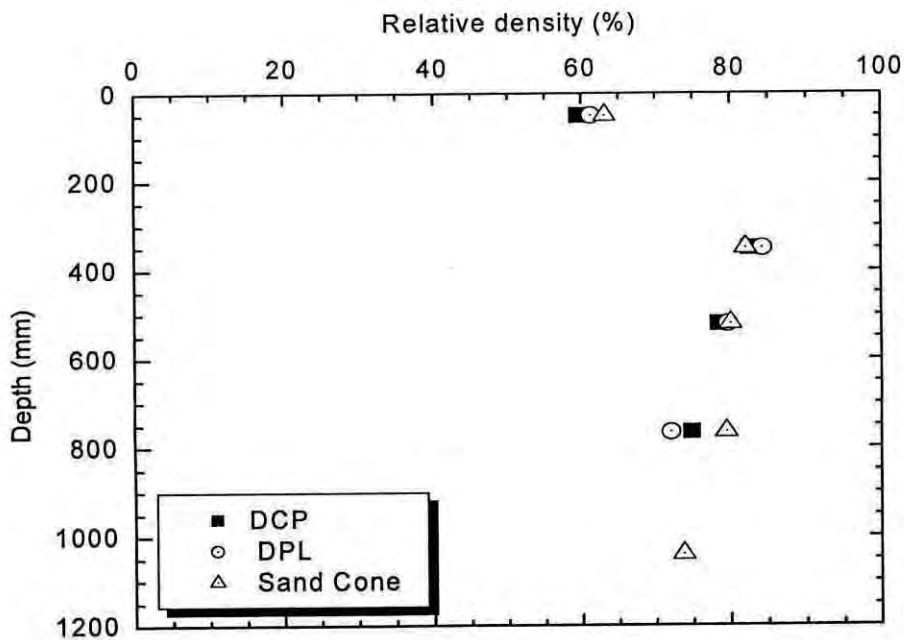


Fig. 4.18: Relative Density vs depth obtained from DCP, DPL and Sand Cone Method (Location 2, Point 1, Jamuna site)

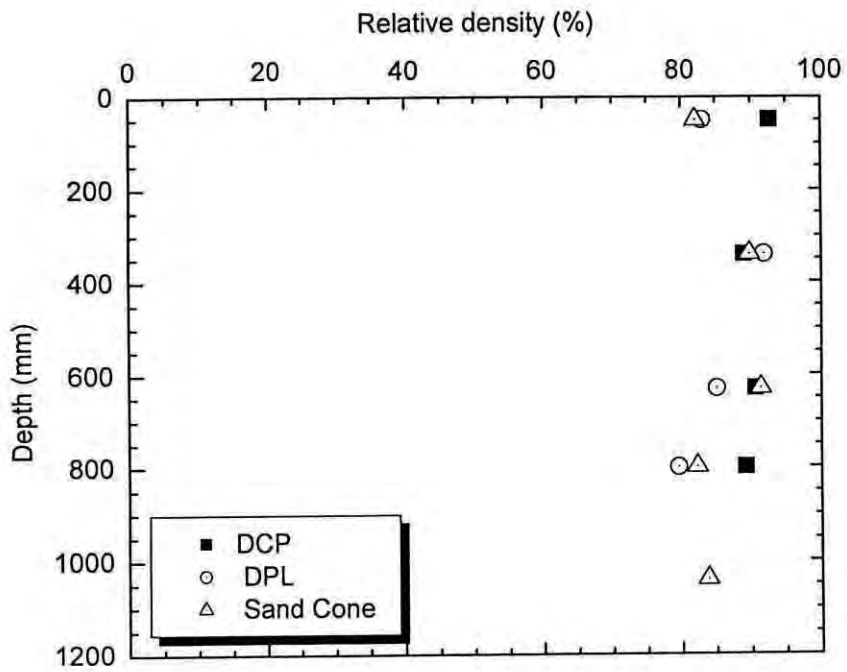


Fig. 4.19: Relative Density vs depth obtained from DCP, DPL and Sand Cone Method (Location 1, Point 1, Pangaon site)

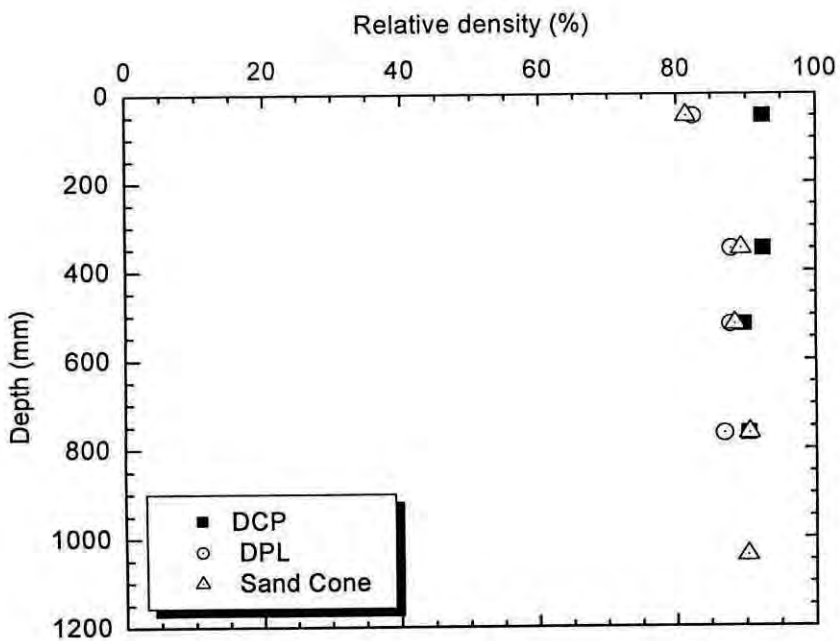


Fig. 4.20: Relative Density vs depth obtained from DCP, DPL and Sand Cone Method (Location 2, Point 1, Pangaon site)

CHAPTER 5 CONCLUSIONS

5.1 General

Azad (2008) calibrated DCP and DPL for two types of sand of Bangladesh. Azad (2008) found good correlations between Relative Density and N_{10} for Jamuna sand and Sylhet sand. He also tried to make a generalized correlation between N_{10} and Relative Density which can be applied for clean sand of any particle size. But in practical field in some case these correlations show more than 100% Relative Density of dredge fill sand which is not acceptable. So, in this study improvement of the correlation was made to overcome this limitation. Here, DCP and DPL tests were performed on a sand deposit of known Relative Density prepared in a calibration chamber. Tests were performed on two types of sand; namely medium sand ($D_{50} = 0.47$ mm) and fine sand ($D_{50} = 0.27$ mm). Here, generalized correlations between Relative Density and $P_{\text{index}}\sqrt{D_{50}}$ were made instead of Relative Density and N_{10} which was made by Azad (2008) for DCP and DPL for clean sand of any particle size. Then the correlations were successfully verified by applying them to determine in situ Relative Density of sand in two dredge fill sites namely Jamuna site and Pangaon site upto 1 m depth.

5.2 Conclusions

The following conclusions are drawn with respect to this experimental study:

- i. A generalized correlation between Relative Density and P_{index} were found which is applicable to clean sand of any particle size.
- ii. Resistance of sand increases exponentially with Relative Density. The larger the particle size greater the resistance to penetration for a certain Relative Density of sand. Denser sand gives more resistance for a specific type of sand.
- iii. The proposed method can be used as an indirect method to determine in situ Relative Density of sand deposit for upto 2 m depth.

5.3 Recommendations for Future Study

The recommendations for future study may be summarized from the lessons of the present study as follows:

- i) P_{index} of DCP and DPL can be correlated with SPT value.
- ii) To prepare sand deposit in calibration chamber instead of air pluviation method another similar study can be done by using wet tamping method.
- iii) The effect of saturation level on dynamic cone resistance can be studied.
- iv) DCP and DPL can be correlated with bearing capacity of dredge fill sand.
- v) DCP and DPL can be correlated with liquefaction potential for different type of sand.

REFERENCES

American Society of Testing Materials (2003). "Standard Test Method for Use of the Dynamic Cone Penetrometer in Shallow Pavement Applications", ASTM D 6951-03, ASTM International, West Conshohocken, PA.

ASTM D1556 – 90. (2006) "Standard Test Method for density & Unit Weight of Soil in Place by the Sand-Cone Method", American Society for Testing and Materials, West Conshohocken, PA 19428-2959, USA.

ASTM D1586 – 99. (2006) "Standard Test Method for Penetration Test and Split-Barrel Sampling of Soils", American Society for Testing and Materials, West Conshohocken, PA 19428-2959, USA.

ASTM D4429 – 93. (2006). "Standard Test Method for CBR (California Bearing Ratio) of Soils in Place", American Society for Testing and Materials, West Conshohocken, PA 19428-2959, USA.

ASTM D6951 – 03. (2006). "Standard Test Method for Use of the Dynamic Cone Penetrometer in Shallow Pavement Applications", American Society for Testing and Materials, West Conshohocken, PA 19428-2959, USA.

Ayers, M. E., Thompson, M. R., and Uzarski, D. R. (1989). "Rapid Shear Strength Evaluation of In Situ Granular Materials". Transp. Res. Rec. 1227, Transp. Res. Board, pp. 134-146.

Bester, M. D., and Hallat, L. (1977). "Dynamic Cone Penetrometer", University of Pretoria, Pretoria.

Burnham, T. and Johnson, D. (1993). "In Situ Foundation Characterization Using the Dynamic Cone Penetrometer", Study No. 9PR3001, Office of Materials Research and Engineering, Minnesota Department of Transportation, USA.

Burnham, T. R. (1997). "Application of Dynamic Cone Penetrometer to Minnesota Department of Transportation Pavement Assessment Procedures", Report No.

MN/RC . 97/19, Minnesota Department of Transportation, St. Paul, MN. 24

Chan, F. W. K., and Armitage, R. J. (1997). "Evaluation of Flexible Pavements in the Middle East", Proceedings of the 8th Inter. Conf. on Asphalt Pavements, August, pp. 459-469.

Chen, D. H., Wang, J-N., and Bilyeu, J. (2001). "Application of Dynamic Cone Penetrometer in Evaluation of Base and Subgrade Layers", Transp. Res. Rec. 1764.

Chen, J., Hossain, M., and LaTorella, T. M. (1999). "Use of Falling Weight Deflectometer and Dynamic Cone Penetrometer in Pavement Evaluation", Transp. Res. Rec. 1655, Trans. Res. Board, pp. 145-151.

Coonse, J. (1999). "Estimating California Bearing Ratio of Cohesive Piedmont Residual Soil Using the Scala Dynamic Cone Penetrometer", MSc Thesis (MSCE), North Carolina State University, Raleigh, N.C., USA.

De Beer, M. (1991). "Use of the Dynamic Cone Penetrometer (DCP) in the Design of Road Structure", Geotechnics in the African Environment, Blight et al (editors), Balkema, Rotterdam, ISBN 90 5410 007 9.

De Beer, M. and Merwe, C. J. (1991). "Use of the Dynamic Cone Penetrometer (DCP) in the Design of Road Structures", Minnesota Department of Transportation, St. Paul, MN.

Ese, Dug, Myre, Jostein, Noss, Per Magne, and Vaernea, Einar. (1994). "The Use of Dynamic Cone Penetrometer (DCP) for Road Strengthening Design in Norway", Proc. Int. Conf. on Bearing Capacity of Rd. and Airfield, pp. 3-22.

Harison, J. R. (1987). "Correlation between California Bearing Ratio and Dynamic Cone Penetrometer Strength Measurement of Soils", Proc. Instn. of Civ. Engrs., London, Part 2, pp. 83-87.

Hassan, A. (1996). "The Effect of Material Parameters on Dynamic Cone Penetrometer Results for Fine-Grained Soils and Granular Materials", Ph.D. Dissertation, Oklahoma State University, Stillwater, Oklahoma.

- Kleyn, E. G. (1975). "The Use of the Dynamic Cone Penetrometer (DCP)", Rep. No. 2/74. Transval Roads Department, South Africa.
- Kleyn, E. G., and Savage, P. E. (1982). "The Application of the Pavement DCP to Determine the Bearing Properties and Performance of the Road Pavements", International Symposium on Bearing Capacity of Roads and Airfields, Trodheim, Norway.
- Livneh, M. (1987). "Validation of Correlations between a Number of Penetration Tests and In Situ California Bearing Ratio Tests", Transp. Res. Rec. 1219. Transportation Research Board, Washington, D.C., pp. 56-67.
- Livneh, M. (2000). "Friction Correction Equation for the Dynamic Cone Penetrometer in Subsoil Strength Testing", Paper Presented at the 79th Transportation Research Board Annual Meeting, Washington, D.C. 27
- Livneh, M., and Ishai, I. (1988). "The Relationship Between In Situ CBR Test and the Various Penetration Tests", Proc. First Int. Conf. on Penetration Testing, Orlando, Fl, pp. 445-452.
- Livneh, M., and Livneh, N. A. (1994). "Subgrade Strength Evaluation with the Extended Dynamic Cone Penetrometer", Proc. 7th Int. IAEG Congress.
- Livneh, M., Ishai, I., and Livneh, N. A. (1992). "Automated DCP Device Versus Manual DCP Device", Rd. and Transport Res., Vol. 1, No. 4.
- Livneh, M., Ishai, I., and Livneh, N. A. (1995). "Effect of Vertical Confinement on Dynamic Cone Penetrometer Strength Values in Pavement and Subgrade Evaluations", Transp. Res. Rec. 1473, pp. 1-9.
- McElvaney, J., and Djatnika, I. (1991). "Strength Evaluation of Lime-Stabilized Pavement Foundations Using the Dynamic Cone Penetrometer", Australian Rd. Res., Volume 21, No. 1, pp. 40-52.
- McGrath, P. (1989). "Dynamic Penetration Testing", Proceedings, Field and Laboratory Testing of Soils for Foundations and Embankments, Trinity College,

Doublin.

McGrath, P. G. et al. (1989). "Development of Dynamic Cone Penetration Testing in Ireland", Proc. Twelfth Int. Conf. on Soil Mechanics and Foundation Engineering. Rio De Janeiro, pp. 271-276.

Meier, R. W., and Baladi, G. Y. (1988). "Cone Index Based Estimates of Soil Strength", Theory and User's Guide for Computer Code CIBESS, Technical Report No. SL-88-11, Waterways Experiment Station, Vicksburg, MS.

Melzer, K. J., and Smolczyk, U. (1982). "Dynamic Penetration Testing-State of the Art Report", Proc. Second European Symposium on Penetration Testing, Amsterdam, Netherlands, pp. 191-202.

Mitchell, J. M. (1988). "New Developments in Penetration Tests and Equipment", Proc. First International Symposium on Penetration Testing. Orlando, FL, pp. 245-262.

Murthy, V. N. S. (1993). "A Text Book of Soil Mechanics & Foundation Engineering", Revised and Enlarged Fourth Edition in SI Units.

Newcomb, D. E., Van-Deusen, D. A., and Burnham, T. R. (1994). "Characterization of Subgrade Soils at the Minnesota Road Research Project", Report No. MN/RD-94/19, Minnesota Department of Transportation, St. Paul, MN.

OVERSEAS ROAD NOTE 31 (1993). "A guide to the structural design of bitumen-surfaced roads in tropical and sub-tropical countries". Overseas Centre, Transportation Research Laboratory, Crowthorne, Berkshire, United Kingdom.

Scala, A. J. (1956). "Simple Methods of Flexible Pavement Design Using Cone Penetrometers", New Zealand Engineering, Vol. 11.

Siekmeier, J., Burnham, T., and Beberg, D. (1998). "Mn/DOT's New Base Compaction Specification Based on the Dynamic Cone Penetrometer", 46th Geotechnical Engineering Conference, University of Minnesota

Sowers, G. and Hedges, C. (1966). "Dynamic Cone for Shallow In-Situ Penetration

Testing”, Vane Shear and Cone Penetration Resistance Testing of In-Situ Soils, ASTM STP 399, American Society for Testing and Materials, pp. 29.

Truebe M. A., and Evans, G. L. (1995). “Lowell Test Road: Helping Improve Road Surfacing Design”, Proc. 6th Int. Conf. on Low-Volume Roads, Minneapolis, Minnesota, Vol. 2, June.

Tumay, M. T. (1994). “Implementation of Louisiana Electric Cone Penetrometer System (LECOPS) For Design of Transportation Facilities Executive Summary”, Louisiana Transportation Research Center, Baton Rouge, LA.

Van Vuuren, D. J. (1969). “Rapid Determination of CBR with the Portable Dynamic Cone Penetrometer”, The Rhodesian Engineer, Vol. 7, No. 5, pp. 852-854.

Appendix A:
DCP & DPL TEST RESULTS

Test Results on Fine Sand in Calibration Chamber

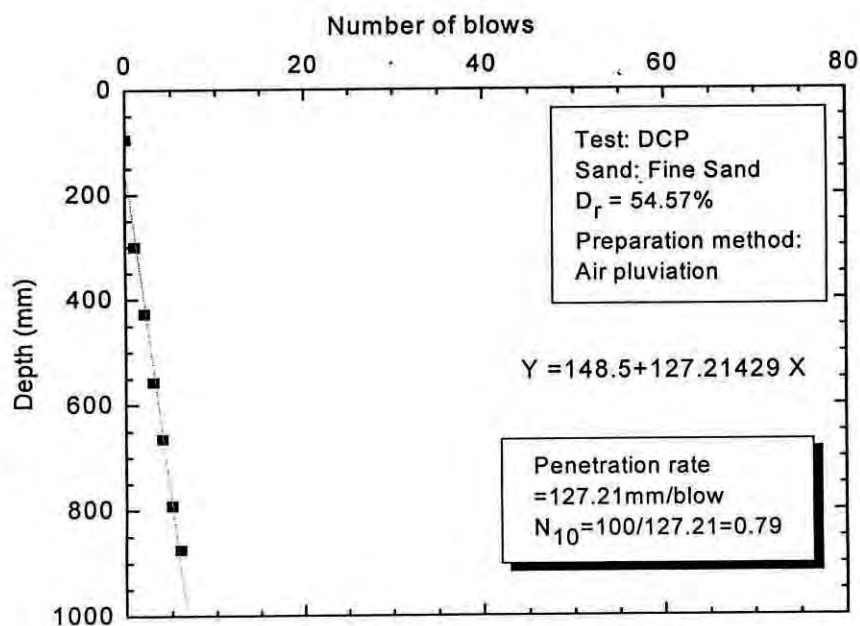


Fig. A.1: Number of blows vs depth plot of DCP test on fine sand in calibration chamber (Relative Density, $D_r = 54.57\%$)

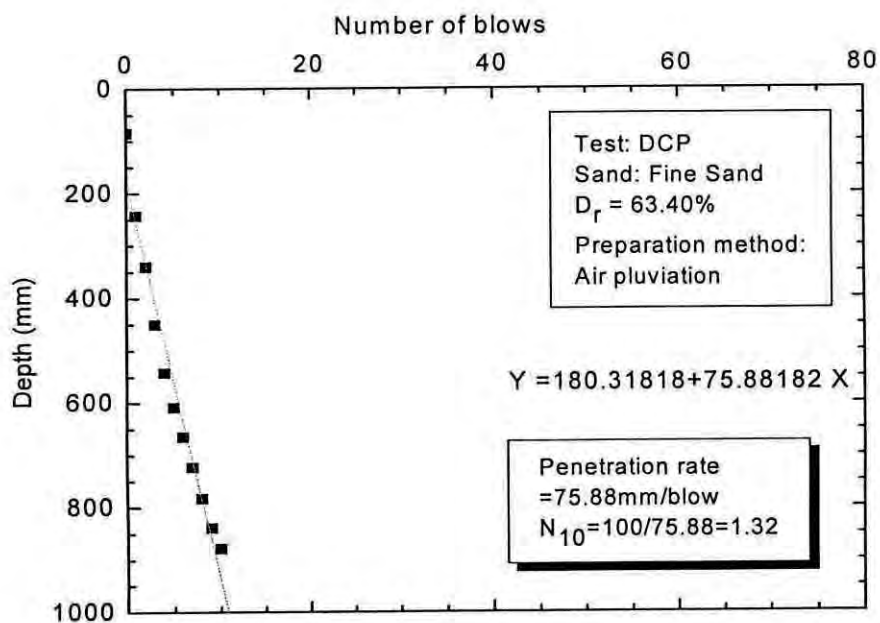


Fig. A.2: Number of blows vs depth plot of DCP test on fine sand in calibration chamber (Relative Density, $D_r = 63.40\%$)

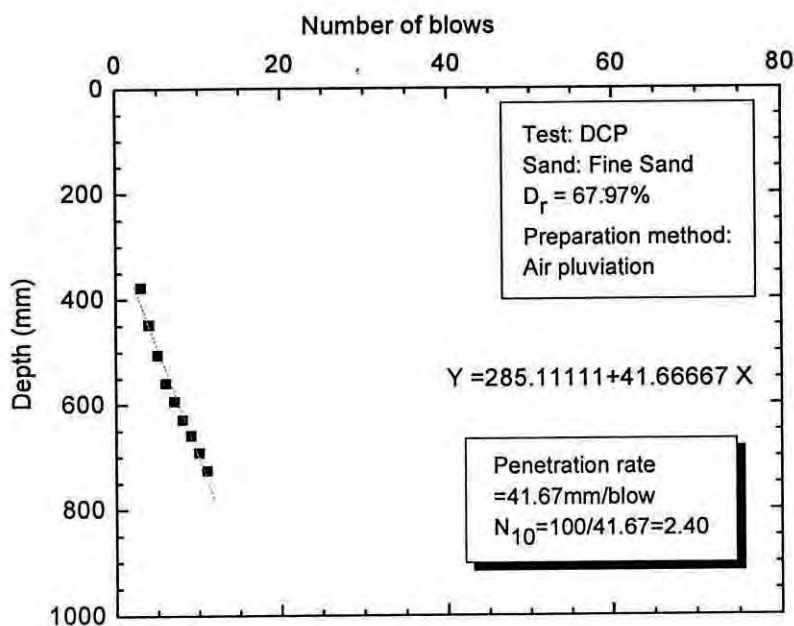


Fig. A.3: Number of blows vs depth plot of DCP test on fine sand in calibration chamber (Relative Density, $D_r = 67.97\%$)

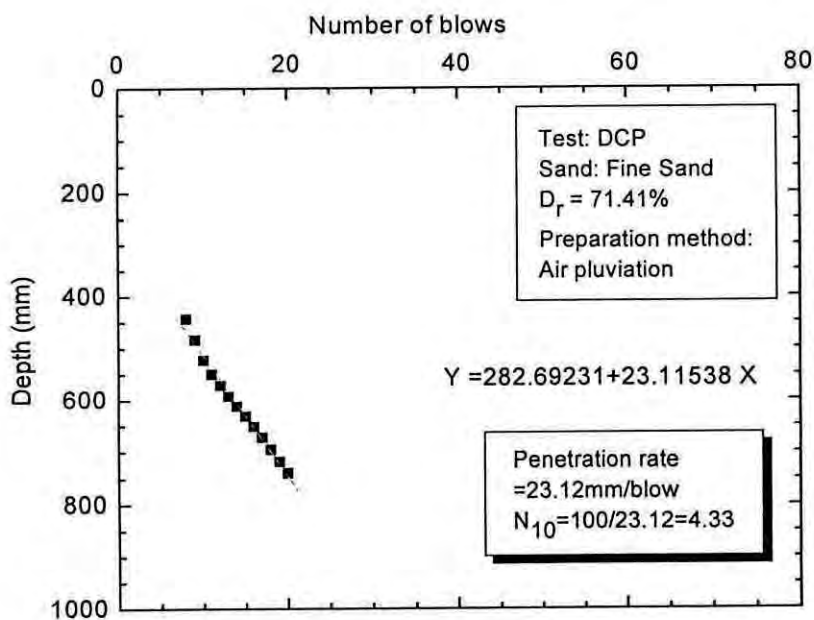


Fig. A.4: Number of blows vs depth plot of DCP test on fine sand in calibration chamber (Relative Density, $D_r = 71.41\%$)

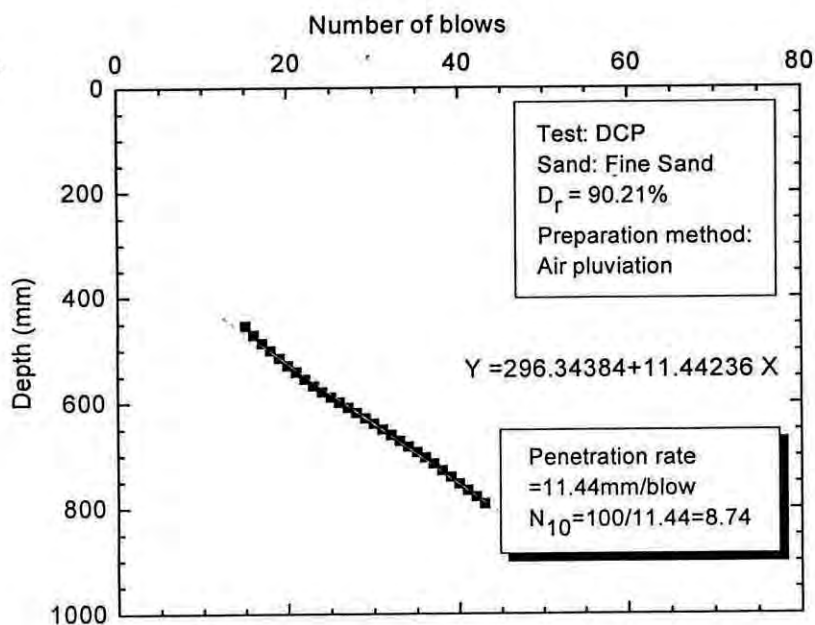


Fig. A.5: Number of blows vs depth plot of DCP test on fine sand in calibration chamber (Relative Density, $D_r = 90.21\%$)

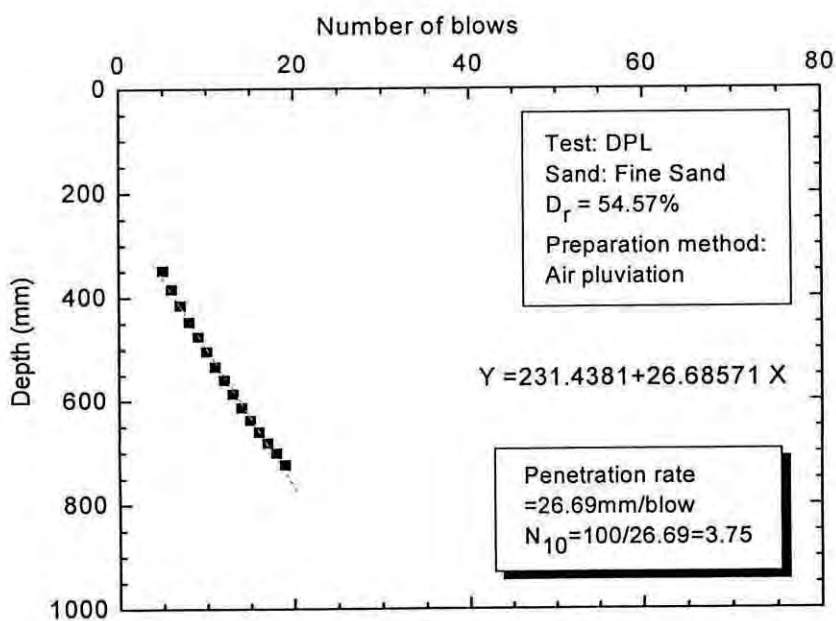


Fig. A.6: Number of blows vs depth plot of DPL test on fine sand in calibration chamber (Relative Density, $D_r = 54.57\%$)

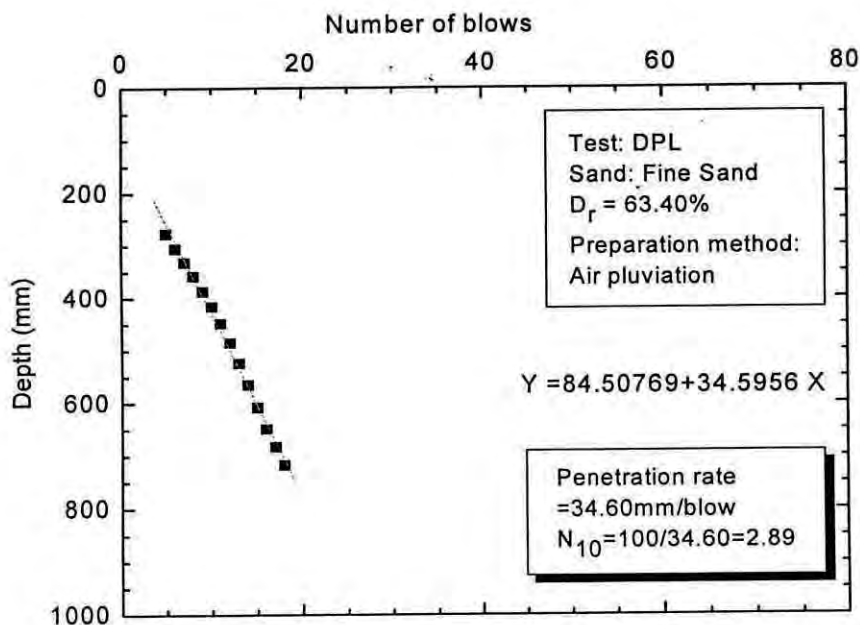


Fig. A.7: Number of blows vs depth plot of DPL test on fine sand in calibration chamber (Relative Density, $D_r = 63.40\%$)

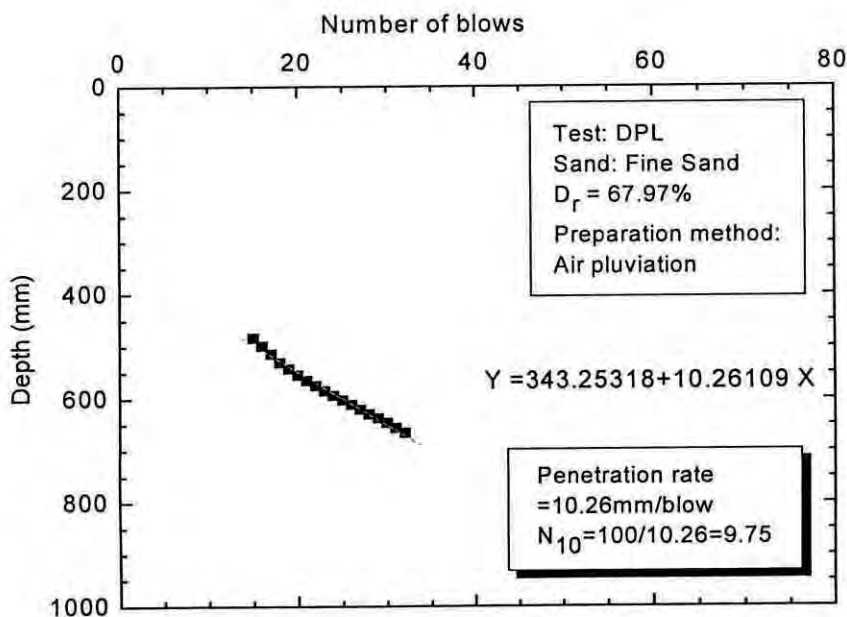


Fig. A.8: Number of blows vs depth plot of DPL test on fine sand in calibration chamber (Relative Density, $D_r = 67.97\%$)

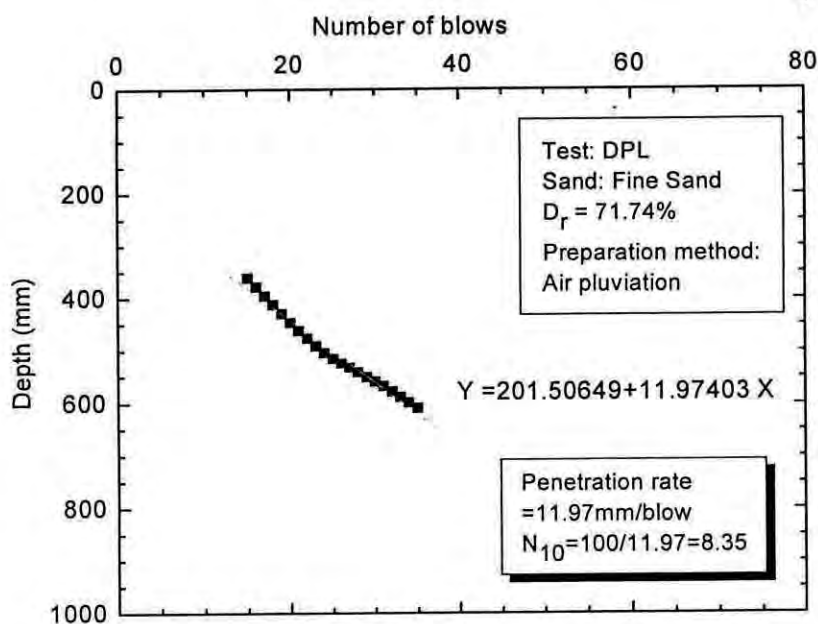


Fig. A.9: Number of blows vs depth plot of DPL test on fine sand in calibration chamber (Relative Density, $D_r = 71.41\%$)

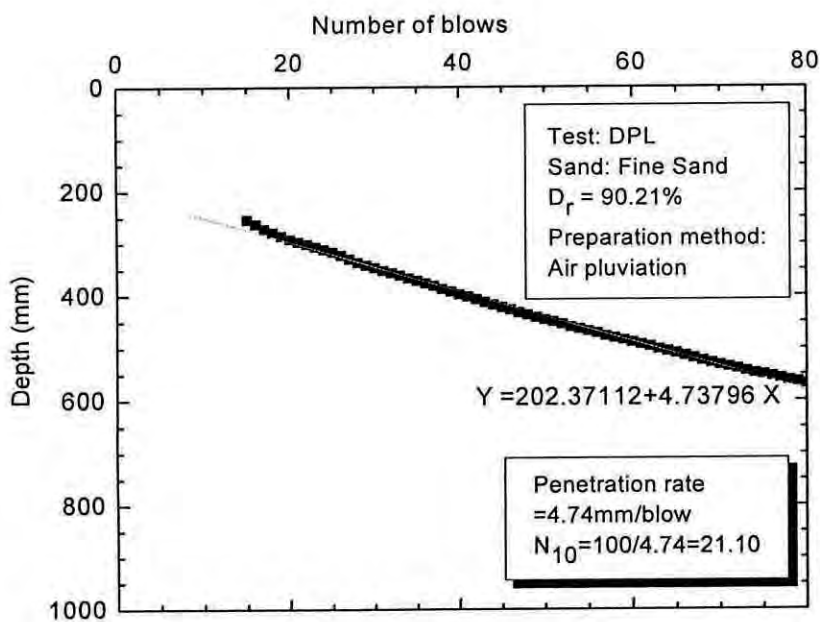


Fig. A.10: Number of blows vs depth plot of DPL test on fine sand in calibration chamber (Relative Density, $D_r = 90.21\%$)

Test Results on Medium Sand in Calibration Chamber

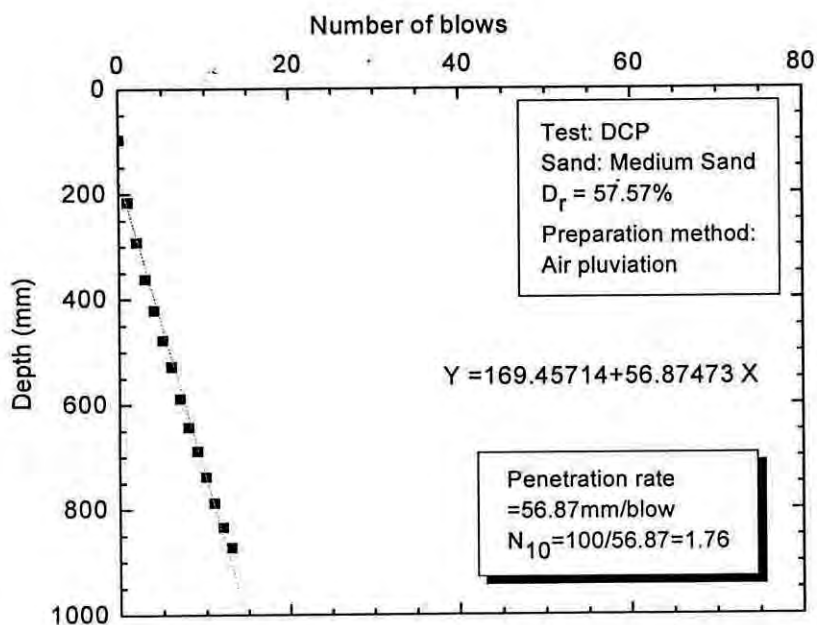


Fig. A.11: Number of blows vs depth plot of DCP test on medium sand in calibration chamber (Relative Density, $D_r = 57.57\%$)

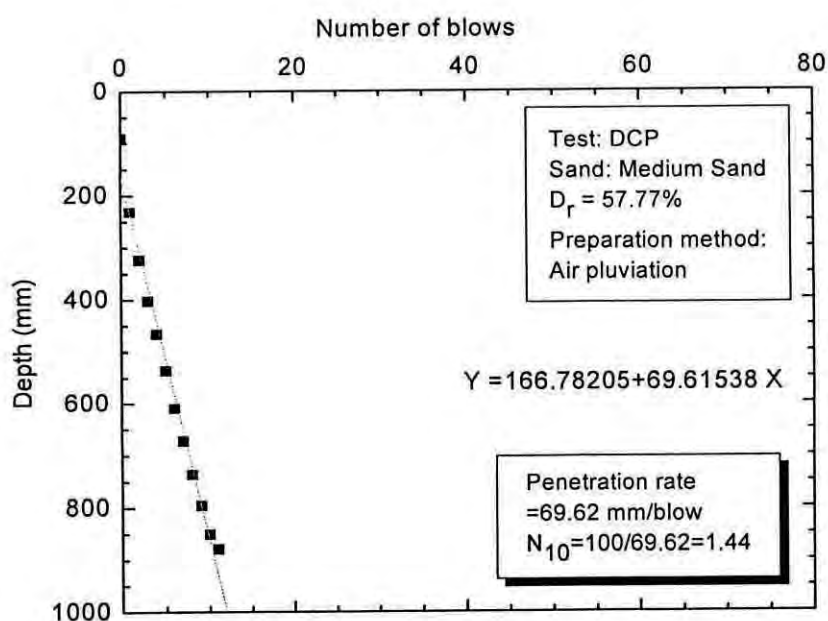


Fig. A.12: Number of blows vs depth plot of DCP test on medium sand in calibration chamber (Relative Density, $D_r = 57.77\%$)

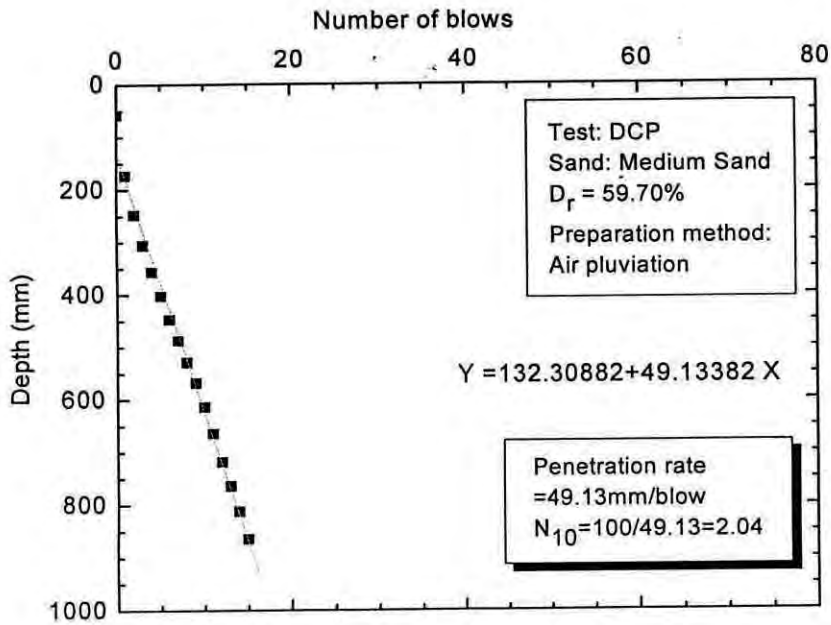


Fig. A.13: Number of blows vs depth plot of DCP test on medium sand in calibration chamber (Relative Density, $D_r = 59.70\%$)

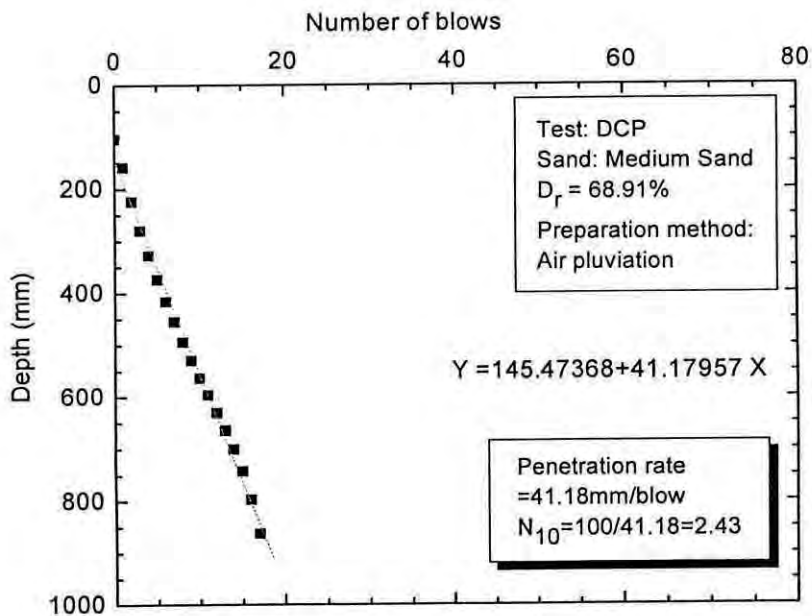


Fig. A.14: Number of blows vs depth plot of DCP test on medium sand in calibration chamber (Relative Density, $D_r = 68.91\%$)

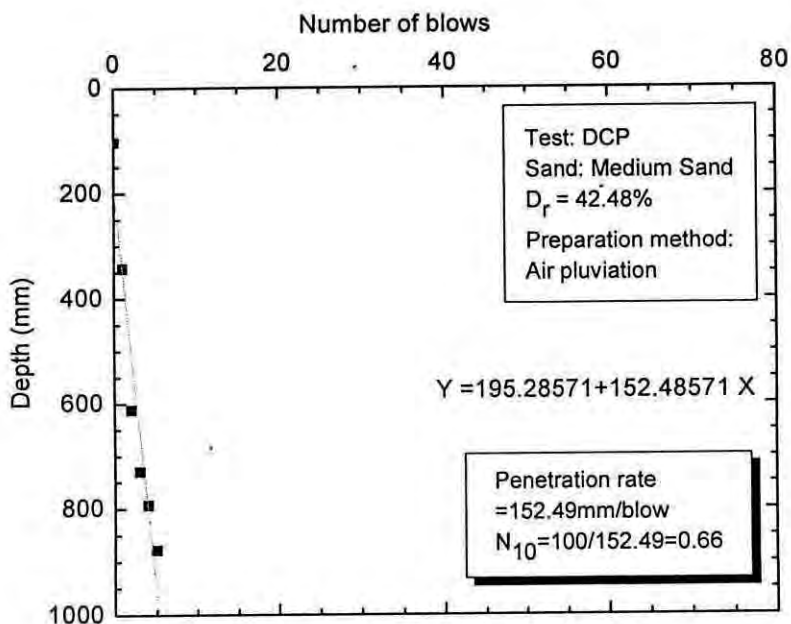


Fig. A.15: Number of blows vs depth plot of DCP test on medium sand in calibration chamber (Relative Density, $D_r = 42.48\%$)

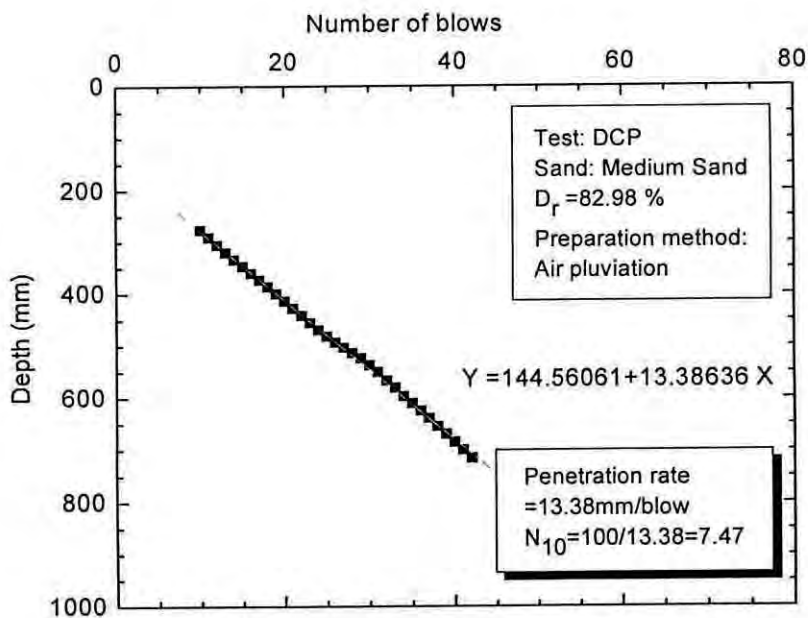


Fig. A.16: Number of blows vs depth plot of DCP test on medium sand in calibration chamber (Relative Density, $D_r = 82.98\%$)

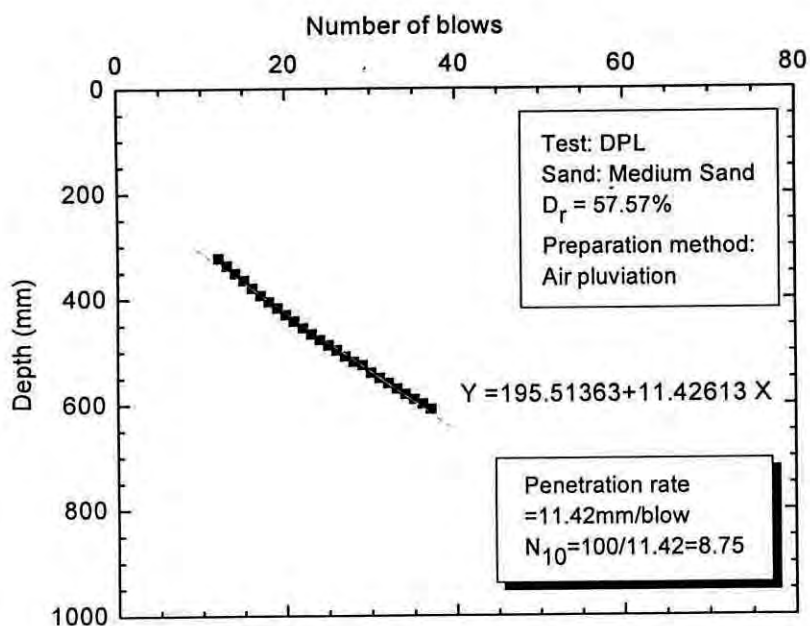


Fig. A.17: Number of blows vs depth plot of DPL test on medium sand in calibration chamber (Relative Density, $D_r = 57.57\%$)

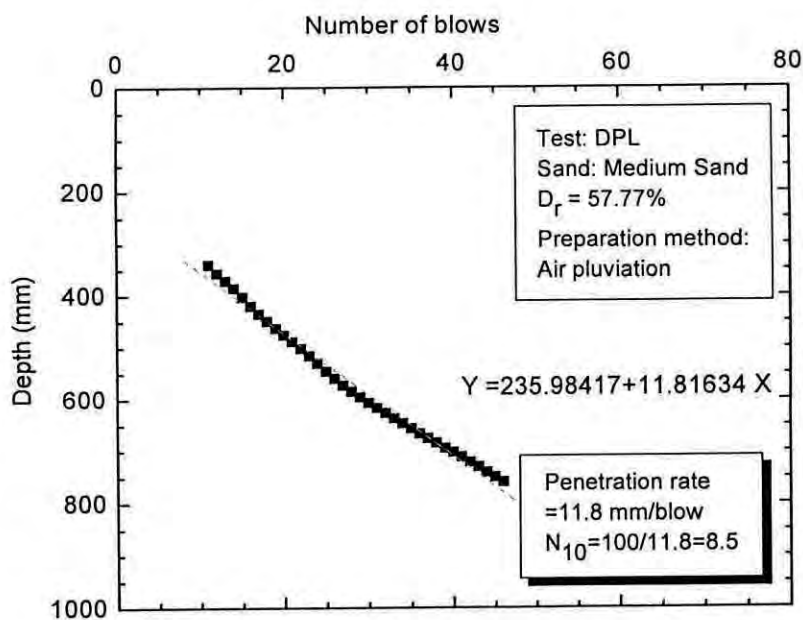


Fig. A.18: Number of blows vs depth plot of DPL test on medium sand in calibration chamber (Relative Density, $D_r = 57.77\%$)

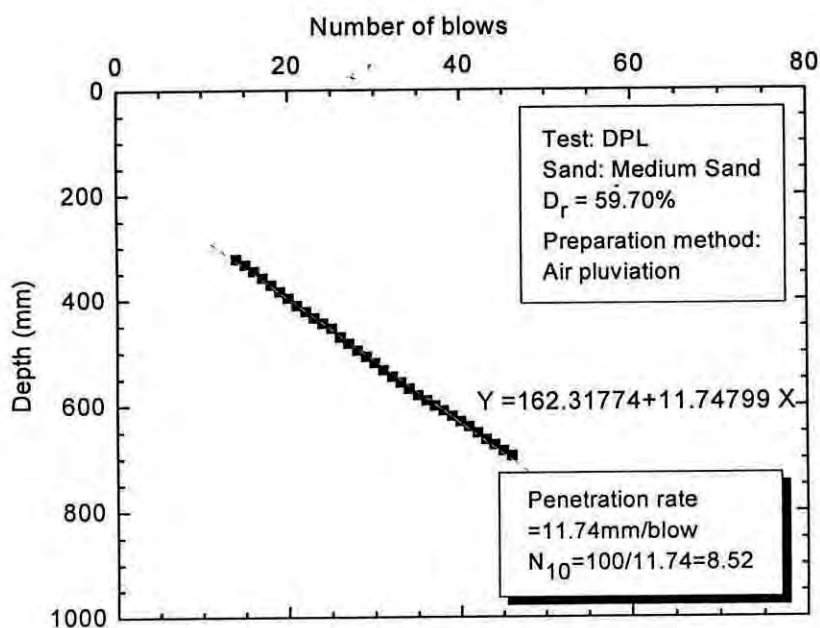


Fig. A.19: Number of blows vs depth plot of DPL test on medium sand in calibration chamber (Relative Density, $D_r = 59.70\%$)

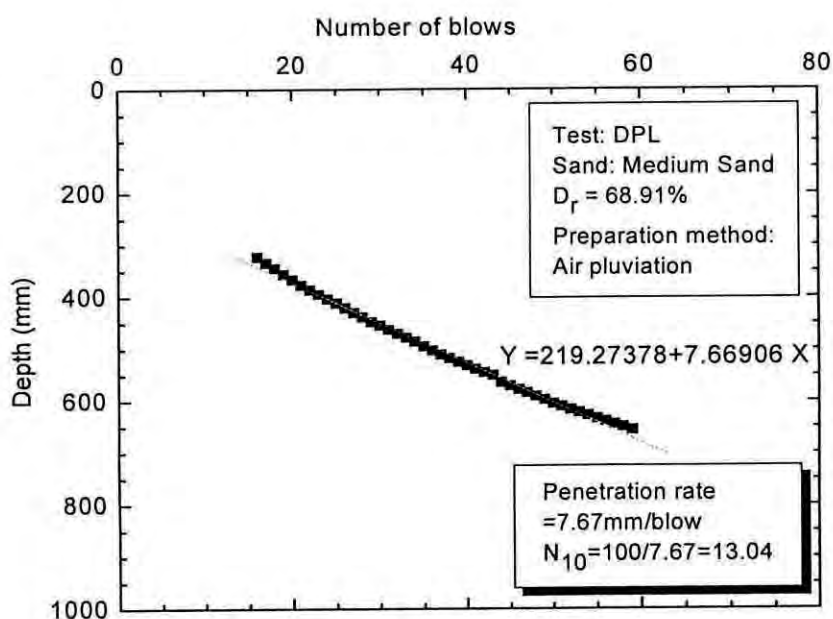


Fig. A.20: Number of blows vs depth plot of DPL test on medium sand in calibration chamber (Relative Density, $D_r = 68.91\%$)

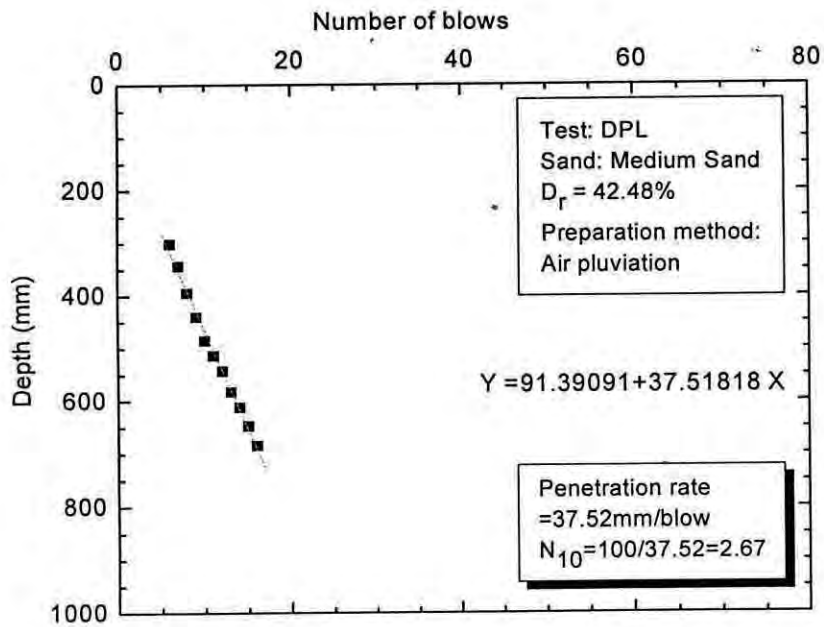


Fig. A.21: Number of blows vs depth plot of DPL test on medium sand in calibration chamber (Relative Density, $D_r = 42.48\%$)

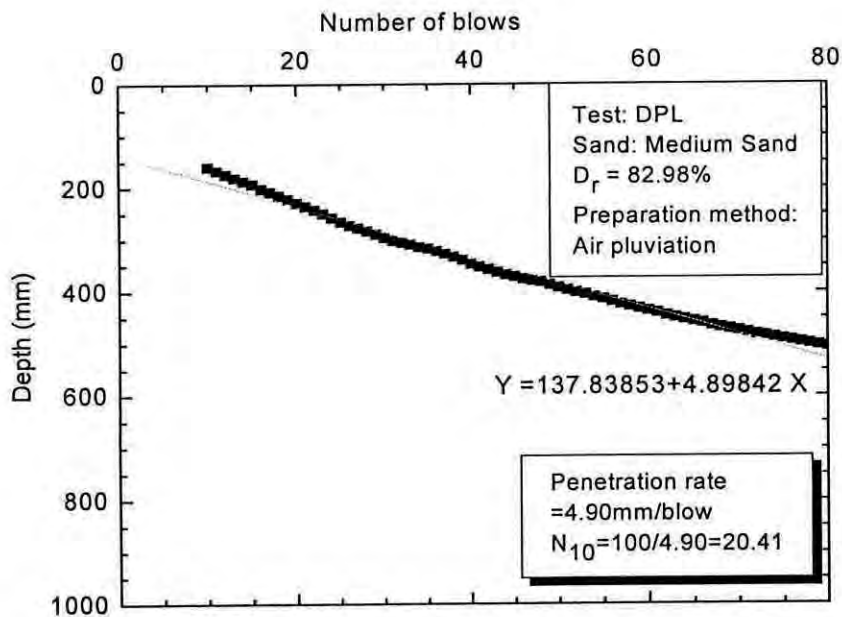


Fig. A.22: Number of blows vs depth plot of DPL test on medium sand in calibration chamber (Relative Density, $D_r = 82.98\%$)

Appendix B:

ASTM Standard of DCP

Designation: D 6951 – 03

Title: Standard Test Method for Use of the Dynamic Cone Penetrometer in Shallow Pavement Applications

1. Scope

1.1 This test method covers the measurement of the penetration rate of the Dynamic Cone Penetrometer with an 8-kg hammer (8-kg DCP) through undisturbed soil and/or compacted materials. The penetration rate may be related to in situ strength such as an estimated in situ CBR (California Bearing Ratio). A soil density may be estimated (Note 1) if the soil type and moisture content are known. The DCP described in this test method is typically used for pavement applications.

1.2 The test method provides for an optional 4.6-kg sliding hammer when the use of the 8-kg sliding mass produces excessive penetration in soft ground conditions.

2. Terminology

2.1 Definitions of Terms Specific to This Standard:

2.1.1 *8-kg DCP dynamic cone penetrometer with an 8 kg hammer* (see Fig. 1)—a device used to assess the in situ strength of undisturbed soil and/or compacted materials.

2.1.2 *Sliding attachment* (see Fig. 1)—an optional device used in reading the distance the DCP tip has penetrated. It may be fastened to the anvil or lower rod to hold/slide along a separate measuring rod or it may be fastened to the separate rod and slide along a graduated drive rod.

3. Summary of Test Method

3.1 The operator drives the DCP tip into soil by lifting the sliding hammer to the handle then releasing it. The total penetration for a given number of blows is measured and recorded in mm/blow, which is then used to describe stiffness, estimate an in situ CBR strength from an appropriate correlation chart, or other material characteristics.

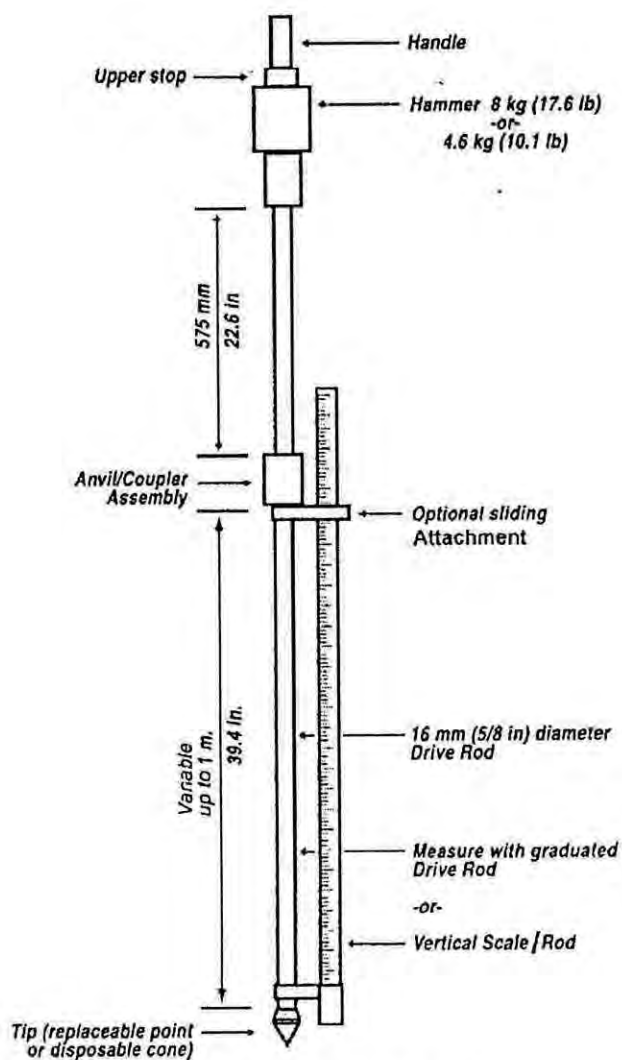


FIG. 1 Schematic of DCP Device

FIG. 1 Schematic of DCP Device

4. Significance and Use

4.1 This test method is used to assess in situ strength of undisturbed soil and/or compacted materials. The penetration rate of the 8-kg DCP can be used to estimate in-situ CBR (California Bearing Ratio), to identify strata thickness, shear strength of strata, and other material characteristics.

4.1.1 Other test methods exist for DCPs with different hammer weights and cone tip sizes, which have correlations that are unique to the instrument.

4.2 The 8-kg DCP is held vertically and therefore is typically used in horizontal construction applications, such as pavements and floor slabs.

4.3 This instrument is typically used to assess material properties down to a depth of 1000-mm (39-in.) below the surface. The penetration depth can be increased using drive rod extensions. However, if drive rod extensions are used, care should be taken when using correlations to estimate other parameters since these correlations are only appropriate for specific DCP configurations. The mass and inertia of the device will change and skin friction along drive rod extensions will occur.

4.4 The 8-kg DCP can be used to estimate the strength characteristics of fine- and coarse-grained soils, granular construction materials and weak stabilized or modified materials. The 8-kg DCP cannot be used in highly stabilized or cemented materials or for granular materials containing a large percentage of aggregates greater than 50-mm (2-in.).

4.5 The 8-kg DCP can be used to estimate the strength of in situ materials underlying a bound or highly stabilized layer by first drilling or coring an access hole.

NOTE 1—The DCP may be used to assess the density of a fairly uniform material by relating density to penetration rate on the same material. In this way under compacted or “soft spots” can be identified, even though the DCP does not measure density directly.

4.5.1 A field DCP measurement results in a field or in situ CBR and will not normally correlate with the laboratory or soaked CBR of the same material. The test is thus intended to evaluate the in situ strength of a material under existing field conditions.

5. Apparatus

5.1 The 8-kg DCP is shown schematically in Fig. 1. It consists of the following components: a 15.8-mm ($\frac{5}{8}$ -in.) diameter steel drive rod with a replaceable point or disposable cone tip, an 8-kg (17.6-lb) hammer which is dropped a fixed height of 575-mm (22.6-in.), a coupler assembly, and a handle. The tip has an included angle of 60 degrees and a diameter at the base of 20-mm (0.79-in.). (See Fig. 2.)

5.1.1 The apparatus is typically constructed of stainless steel, with the exception of the replacement point tip, which may be constructed from hardened tool steel or a similar material resistant to wear.

5.2 The following tolerances are recommended:

“METHOD ST6: Measurement of the In Situ Strength of Soils by the Dynamic Cone Penetrometer (DCP), Special Methods for Testing Roads,” Draft TMH6, Technical Methods for Highways (TMH), Pretoria, South Africa, ISBN 0 7988 2289 9, 1984, p. 20.

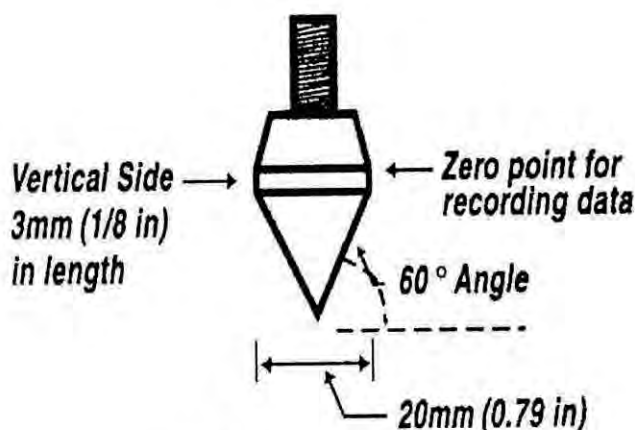


FIG. 2 Replaceable Point Tip

5.2.1 Hammer weight-measurement of 8.0-kg (17.6-lb); tolerance is 0.010-kg (0.022-lb),

5.2.2 Hammer weight-measurement of 4.6-kg (10.1-lb.); tolerance is 0.010-kg (0.022-lb),

5.2.3 Drop of hammer-measurement of 575-mm (22.6-in.); tolerance is 1.0-mm (0.039-in.),

5.2.4 Tip angle measurement of 60 degrees included angle; tolerance is 1 degree, and

5.2.5 Tip base diameter measurement of 20-mm (0.790-in.); tolerance is 0.25-mm (0.010-in.)

NOTE 2—A disposable cone tip may be used. The disposable cone tip is held in place with an o-ring, which allows the cone tip to be easily detached when the drive rod is pulled upward after completion of the test. The disposable cone tip is shown schematically in Fig. 3.

5.3 In addition to the DCP, the following equipment is needed:

5.3.1 Tools for assembling the DCP,

5.3.2 Lubricating Oil,

5.3.3 Thread Locking Compound, and

5.3.4 Data Recording form (see Table 1).

TABLE 1: DCP Example Data Sheet

Project: Forest Service Road Location: STA 30+50. 1 M RT of C/L Depth of zero point below Surface:0 Material Classification: GW/CL Pavement condition: Not applicable				Date: 7 July 2001 Personnel: JLS & SOT. Hammer Weight: 8-kg (17.6-lb) Weather: Overcast. 25°C. (72°F) Water Table Depth: Unknown			
Number of Blows ^A	Cumulative Penetration (mm) ^B	Penetration Between Reading (mm) ^C	Penetration per blow (mm) ^D	Hammer Factor ^E	DCP Index mm/blow ^F	CB R % ^G	Moisture % ^H
0	0	--	--	--	--	--	
5	25	25	5	1	5	50	
5	55	30	6	1	6	40	
15	125	70	5	1	5	50	
10	175	50	5	1	5	50	
5	205	30	6	1	6	40	
5	230	25	5	1	5	50	
10	280	50	5	1	5	50	
5	310	30	6	1	6	40	
5	340	30	6	1	6	40	
5	375	35	7	1	7	35	
5	435	60	12	1	12	18	

^A Number of hammer blows between test readings.

^B Cumulative penetration after each set of hammer blows.

^C Difference in cumulative penetration (Footnote B) between readings.

^D Footnote C divided by Footnote A.

^E Enter 1 for 8-kg (17.6-lb) hammer; 2 for 4.6-kg (10.1-lb) hammer.

^F Footnote D 3 Footnote E.

^G From CBR versus DCP Index correlation.

^H % Moisture content when available.

5.4 Depending on the circumstances, the following equipment may also be needed or is recommended:

5.4.1 A vertical scale graduated using increments of 1.0-mm (0.04-in.), or measuring rod longer than the longest drive rod if the drive rod(s) are not graduated,

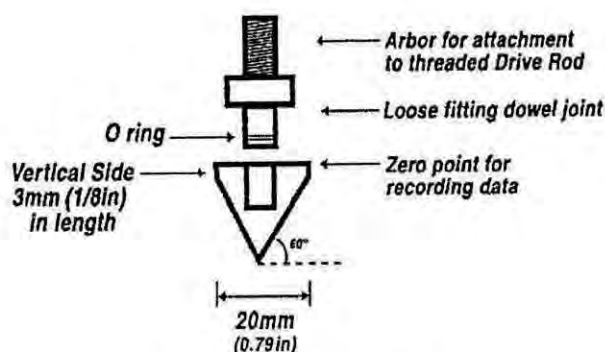


FIG. 3 Disposable Cone Tip

- 5.4.2 An optional sliding attachment for use with a separate scale or measuring rod,
- 5.4.3 A rotary hammer drill or coring apparatus capable of drilling a minimum diameter hole of 25-mm (1-in.). A larger hole may be required depending on the underlying material or the need for addition tests or sampling,
- 5.4.4 A wet/dry vacuum or suitable alternative to remove loose material and fluid if an access hole is made before testing,
- 5.4.5 Field power supply to power items in 5.4.3 and 5.4.4,
- 5.4.6 Disposable cone tips,
- 5.4.7 Dual mass hammer (see Fig. 4), and
- 5.4.8 Extraction jack, recommended if disposable cone tips are not used (see Fig. 5).

NOTE 3—A 4.6-kg (10.1-lb) hammer (see Fig. 4) may be used in place of the 8-kg (17.6-lb) hammer provided that the standard drop height is maintained. The 4.6-kg (10.1-lb) hammer is used in weaker materials where the 8-kg (17.6-lb) hammer would produce excessive penetration.

NOTE 4—An automated version of the DCP (ADCP) may be used provided all requirements of this standard with respect to the apparatus and procedure are met.

NOTE 5—An automated data collection system may be used provided it measures and records to the nearest 1-mm (0.04-in.) and does not interfere with the operation/results of the device.

6. Procedure

6.1 *Equipment Check*—Before beginning a test, the DCP device is inspected for fatigue-damaged parts, in particular the coupler and handle, and excessive wear of the drive rod and replaceable point tip. All joints must be securely tightened including the coupler assembly and the replaceable point tip (or the adapter for the disposable cone tip) to drive rod.

6.2 *Basic Operation*—The operator holds the device by the handle in a vertical or plumb position and lifts and releases the hammer from the standard drop height. The recorder measures and records the total penetration for a given number of blows or the penetration per blow.

6.3 *Initial Reading:*

6.3.1 *Testing a Surface Layer*—The DCP is held vertically and the tip seated such that the top of the widest part of the tip is flush with the surface of the material to be tested. An initial reading is obtained from the graduated drive rod or a separate vertical scale/measuring rod. The distance is measured to the nearest 1-mm (0.04-in.). Some sliding reference attachments allow the scale/measuring rod to be set/marked at zero when the tip is at the zero point shown in Fig. 2.

6.3.2 *Testing below a Bound Layer*—When testing materials underlying a bound layer, a rotary hammer drill or coring apparatus meeting the requirements given in 5.4.3 above is used to provide an access hole to the layer to be tested. Wet coring requires that coring fluid be removed immediately and the DCP test be performed as soon as possible, but not longer than 10 min following completion of the coring operation. The coring fluid must not be allowed to soak into or penetrate the material to be tested. A wet/dry vacuum or suitable alternative is used after completion of drilling or coring to remove loose materials and fluid from the access hole before testing. To minimize the extent of the disturbance from the rotary hammer, drilling should not be taken completely through the bound layer, but stopped short by about 10-to 20-mm. The DCP is then used to penetrate the bottom portion of the bound layer. This can be a repetitive process between drilling and doing DCP tests to determine the thickness of the layer.

6.3.3 *Testing Pavement with Thin Seals*—For pavements with thin seals, the tip is advanced through the seal until the zero point (see Fig. 4) of the tip is flush with the top of the layer to be tested.

6.3.4 Once the layer to be tested has been reached, a reference reading is taken with the zero point at the top of that layer and the thickness of the layer(s) cored through recorded. This reference reading is the point from which the subsequent penetration is measured.

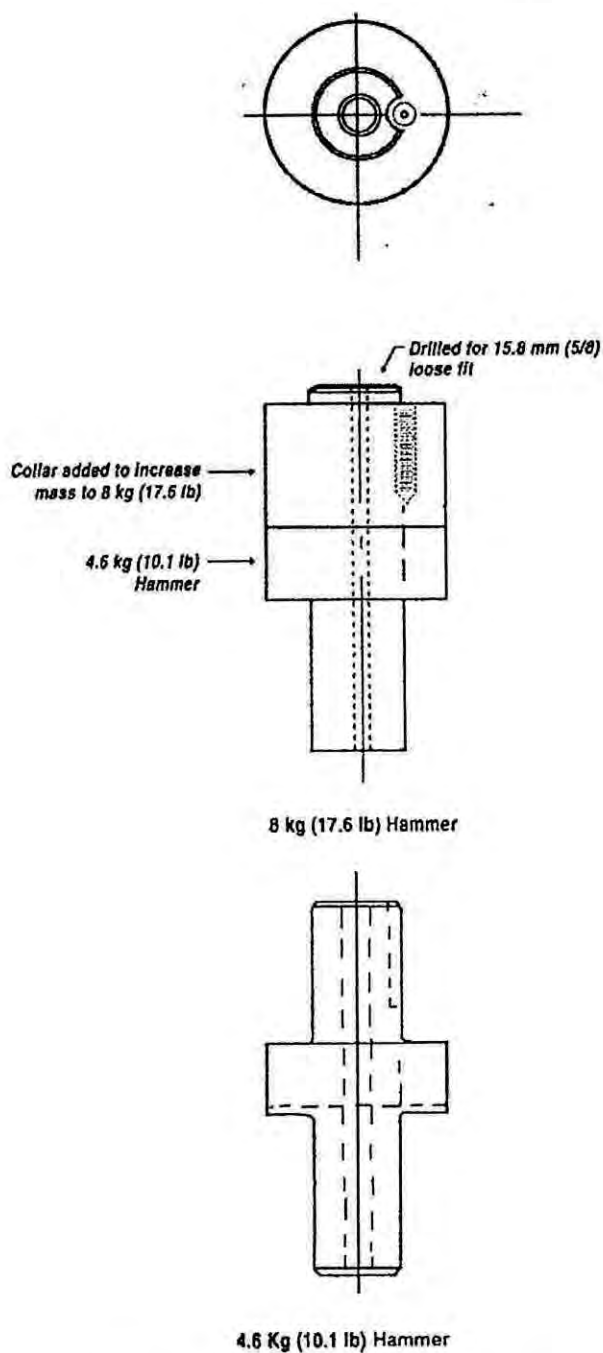


FIG. 4 Schematic of Dual-Mass Hammer

FIG. 4 Schematic of Dual-Mass Hammer

6.4 Testing Sequence:

6.4.1 *Dropping the Hammer*—The DCP device is held in a vertical or plumb position. The operator raises the hammer until it makes only light contact with the handle. The hammer shall not impact the handle when being raised. The hammer is then allowed

to free-fall and impact the anvil coupler assembly. The number of blows and corresponding penetrations are recorded as described in 6.5.

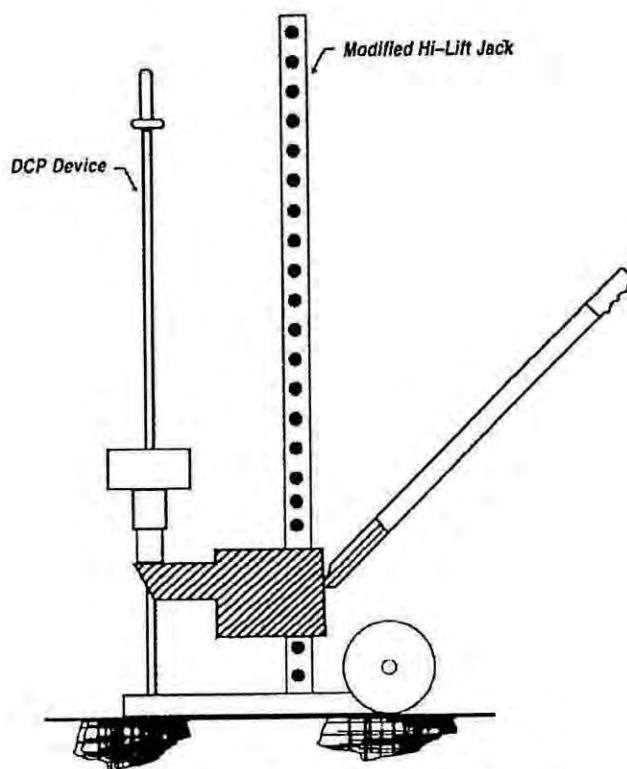


FIG. 5 Schematic of DCP Extraction Jack

6.4.2 *Depth of Penetration*—The depth of penetration will vary with application. For typical highway applications, a penetration less than 900-mm (35-in.) will generally be adequate.

6.4.3 *Refusal*—The presence of large aggregates or rock strata will either stop further penetration or deflect the drive rod. If after 5 blows, the device has not advanced more than 2-mm (0.08-in.) or the handle has deflected more than 75-mm (3-in.) from the vertical position, the test shall be stopped, and the device moved to another test location. The new test location should be a minimum of 300-mm (12-in.) from the prior location to minimize test error caused by disturbance of the material.

6.4.4 *Extraction*—Following completion of the test, the device should be extracted using the extraction jack when using a replaceable point tip. When using a disposable cone, the device is extracted by driving the hammer upward against the handle.

6.5 Data Recording:

6.5.1 A form like the one shown in Table 1 is suggested for data recording. The recorder enters the header information before the test. The actual test data are recorded in column 1 (Number of Blows) and column 2 (Cumulative Penetration in mm); if the moisture content is available, it is entered in column 8. When testing a subsurface layer through a drilled or cored access hole, the first reading corresponds to the referenced reading at the top of the layer to be tested as per 6.3.2. The number of blows between readings may be varied depending on the resistance of the material. Normally readings will be taken after a fixed number of blows, that is, 1 blow for soft material, 5 blows for "normal" materials and 10 blows for very resistive materials. The penetration to the nearest 1-mm (0.04in.) corresponding to a specific number of blows is recorded. A reading is taken immediately when the material properties or penetration rate change significantly.

TABLE 2 Tabulated Correlation of CBR versus DCP Index³

DCP Index mm/blow	CBR %	DCP Index mm/blow	CBR %	DCP Index mm/blow	CBR %
<3	100	39	4.8	69-71	2.5
3	80	40	4.7	72-74	2.4
4	60	41	4.6	75-77	2.3
5	50	42	4.4	78-80	2.2
6	40	43	4.3	81-83	2.1
7	35	44	4.2	84-87	2.0
8	30	45	4.1	88-91	1.9
9	25	46	4.0	92-96	1.8
10-11	20	47	3.9	97-101	1.7
12	18	48	3.8	102-107	1.6
13	16	49-50	3.7	108-114	1.5
14	15	51	3.6	115-121	1.4
15	14	52	3.5	122-130	1.3
16	13	53-54	3.4	131-140	1.2
17	12	55	3.3	141-152	1.1
18-19	11	56-57	3.2	153-166	1.0
20-21	10	58	3.1	166-183	0.9
22-23	9	59-60	3.0	184-205	0.8
24-26	8	61-62	2.9	206-233	0.7
27-29	7	63-64	2.8	234-271	0.6
30-34	6	65-66	2.7	272-324	0.5
35-38	5	67-68	2.6	>324	<0.5

7. Calculations and Interpretation of Results

7.1 The estimated in situ CBR is computed using the DCP index (column 6, Table 1) and Table 2 for each set of readings. The penetration per blow may then be plotted

against scale reading or total depth. The penetration per blow is then used to estimate in situ CBR or shear strength using the appropriate correlation. For example, the correlation of penetration per blow (DCP) in Table 2 is derived from the equation $CBR = 292 / DCP^{1.12}$ recommended by the US Army Corps of Engineers.³ This equation is used for all soils except for CL soils below

³ Webster, S. L., Grau, R. H., and Williams, T. P., "Description and Application of Dual Mass Dynamic Cone Penetrometer," *Report GL-92-3*, Department of the Army, Washington, DC, May 1992, p. 19.

CBR 10 and CH soils. For these soils, the following equations are recommended by the US Army Corps of Engineers:⁴

CL soils CBR < 10: $CBR = 5 / \sim 0.017019 * DCP!^2$

CH soils: $CBR = 5 / 0.002871 * DCP$

7.1.1 Selection of the appropriate correlation is a matter of professional judgment.

7.2 If a distinct layering exists within the material tested, a change of slope on a graph of cumulative penetration blows versus depth will be observed for each layer. The exact interface is difficult to define because, in general, a transition zone exists between layers. The layer thickness can be defined by the intersection of the lines representing the average slope of adjacent layers. Once the layer thicknesses have been defined, the average penetration rate per layer is calculated.

8. Report

8.1 The report should include all the information as shown in Table 1. The relationship used to estimate the in situ CBR values should also be included.

9. Precision and Bias

9.1 *Precision*—The within-field-laboratory repeatability standard deviation has been determined to be less than 2 mm/blow.⁵ It is not possible to determine reproducibility limits for this field test, which is destructive in nature and the sample is not homogeneous and cannot be replicated in moisture and density in another laboratory.

NOTE 6—The repeatability study⁵ is on granular materials and would correspond to approximately 20 percent or less if expressed as a percentage.

9.2 *Bias*—No statement is being made as to the bias of the test method at the present time.

10. Keywords

10.1 ADCP; aggregate base testing; California bearing ratio; CBR; DCP; disposable cones; dual-mass hammer; dynamic cone penetrometer; in situ testing; paving material testing; shear strength; subgrade testing

BIBLIOGRAPHY

⁴ Webster, S. L., Brown, R. W., and Porter, J. R., "Force Projection Site Evaluation Using the Electric Cone Penetrometer (ECP) and the Dynamic Cone Penetrometer (DCP)," *Technical Report No. GL-94-17*, Air Force Civil Engineering Support Agency, U.S. Air Force, Tyndall Air Force Base, FL, April 1994.

⁵ Burnham, T. R., "Application of Dynamic Cone Penetrometer to Minnesota Department of Transportation Pavement Assessment Procedures," *MN/RC-97/19*, Minnesota Department of Transportation, Saint Paul, MN, 1997, p. 37.

(1) Ayers, M. E., "Rapid Shear Strength of In Situ Granular Materials Utilizing the Dynamic Cone Penetrometer," Ph.D. Theses, University of Illinois, Urbana, IL, 1990.

(2) De Beer, M., Kleyn, E. G., and Savage P. F., "Towards a Classification System for the Strength-Balance of Thin Surfaced Flexible Pavements," *Proceedings of the 1988 Annual Transportation Convention (ATC '88), Session S.443*, Vol 3D, Paper 3D-4, Pretoria, July 1988.

(3) De Beer, M., "Dynamic Cone Penetrometer (DCP) Aided Evolution of the Behaviour of Pavements with Lightly Cementitious Layers,"

Division of Roads and Transport Technology, Research Report DPVT-37, CSIR, Pretoria, South Africa, April 1989.

(4) De Beer, M., Kleyn, E. G., and Savage, P. F., "Advances in Pavement Evaluation and Overlay Design with the Aid of the Dynamic Cone Penetrometer (DCP)," *2nd International Symposium on Pavement Evaluation and Overlay Design, 11th to 15th September 1989, Rio de Janeiro, Brazil.*

(5) De Beer, M., "Use of the Dynamic Cone Penetrometer (DCP) in the Design of Road Structures," *Tenth African Regional Conference on Soil Mechanics and Foundation Engineering, Maseru, Lesotho, September 1991. Geotechnics in the African Environment, Blight, et al (eds.), Balkema, Rotterdam, Vol 1, 1991, pp. 167-183.* Also in *Research Report DPVT-187, Roads and Transport Technology, CSIR, South Africa.*

(6) De Beer, M., "Use of the Dynamic Cone Penetrometer (DCP) in the Design of Road Structures," *Research Report DPVT-18, Roads and Transport Technology, CSIR, South Africa, 1991, p. 30.*

(7) De Beer, M., "Dynamic Cone Penetrometer (DCP), the Development of DCP Pavement Technology in South Africa," Session 7, course notes from RSA/US Pavement Technology Workshop, at Richmond Field Station, University of California, Berkeley, March 2000.

(8) Kessler, K.C., *Dynamic Cone Penetrometer User's Manual.* Kessler Soils Engineering Products, Inc., January 2001, Springfield, VA.

(9) Kleyn, E. G., "The Use of the Dynamic Cone Penetrometer (DCP)," *Report 2/74, Transvaal Roads Department, Pretoria, South Africa, July 1975, p. 35.*

(10) Kleyn, E. G., Maree, J. H., and Savage, P. F., "Application of a Portable Pavement Dynamic Cone Penetrometer to Determine in situ Bearing Properties of Road Pavement Layers and Subgrades in South Africa," *ESOPT 11, Amsterdam, Netherlands, 1982.*

- (11) Kleyn, E. G., and Savage, P. F., "The Application of the Pavement DCP to Determine the Bearing Properties and Performance of Road Pavements," *International Symposium on Bearing Capacity of Roads and Airfields*, Trondheim, Norway, 1982.
- (12) Kleyn, E. G., Van Heerden, M. J. J., and Rossouw, A. J., "An Investigation to Determine the Structural Capacity and Rehabilitation Utilization of a Road Pavement Using the Pavement Dynamic Cone Penetrometer," *International Symposium on Bearing Capacity of Roads and Airfields*, Trondheim, Norway, 1982.
- (13) Kleyn, E. G., and Van Heerden, M. J. J., "Using DCP Soundings to Optimize Pavement Rehabilitation," *Annual Transport Convention, Session G: Transport Infrastructure*, Johannesburg, South Africa, 1983.
- (14) Kleyn, E. G., in Afrikaans, "Aspects of Pavement Evaluation and Design as Determined with the Dynamic Cone Penetrometer (DCP)," M. Eng. Thesis, University of Pretoria, Pretoria, South Africa, May 1984. (Approximately 13000 words, 51 Figures and 1 photo.)
- (15) Kleyn, E. G., Van Van Zyl, G. D., "Application of the Dynamic Cone Penetrometer (DCP) to Light Pavement Design," *Proceedings of First International Symposium on Penetration Testing, Orlando Florida*, A.A. Balkema Publishers, Rotterdam, Netherlands, 1988, pp. 435-444.
- (16) Livneh, M., "The Relationship Between In Situ CBR Test and Various Penetration Test," *Proceedings of the First Symposium on Penetration Testing, Orlando, Florida*, A.A. Balkema Publishers, Rotterdam, Netherland, 1988.
- (17) Livneh, M., "Validation of Correlations Between a Number of Penetrations Tests and In Situ California Bearing Ratio Tests," *Transportation Research Record 1219*, Transportation Research Record, Washington, DC, 1989.

- (18) Livneh, M., "The Israeli Experience with the Regular and Extended Dynamic Cone Penetrometer for Pavement and Subsoil Strength Evaluation, Nondistructive Testing of Pavements and Backcalculation of Moduli," *ASTM STP 1375*, S. D. Tayabji and E. O. Lukanen, Eds., American Society for Testing and Materials, West Conshohocken, PA, 1999.
- (19) "METHOD ST6: Measurement of the In Situ Strength of soils by the Dynamic Cone Penetrometer (DCP), Special Methods for Testing Roads," Draft TMH6, Technical Methods for Highways (TMH), ISBN 0 7988 2289 9, 1984, pp. 19-24.
- (20) Sampson, L. R., and Netterberg, F., "Effect of Material Quality on the Relationship Between nDCP DN-Value and CBR," *Proceedings of the Annual Transportation Convention, Pretoria, South Africa*, Vol 5B, Paper #3, 1990, p. 12.
- (21) Scala, A. J., "Simple Methods of Flexible Pavement Design Using Cone Penetrometers," *Proceedings of the Second Australian Soil Mechanics Conference, Christ Church, New Zealand, New Zealand Engineer*, 11(2), 1956, pp. 34-44.
- (22) Siekmeier, J. A., Young, D., and Beberg, D., "Comparison of the Dynamic Cone Penetrometer with Other Tests During Subgrade and Granular Base Characterization in Minnesota," *Nondestructive Testing of Pavements and Backcalculation of Moduli: Third Volume, ASTM STP 1375*, S. D. Tayabji and E. O. Lukanen, Eds., American Society for Testing and Materials, West Conshohochen, PA, 1999.
- (23) Stephanos, G., Stanglerat, G., Bergdahl, V., and Melzer, K. J., "Dynamic Probing (DP): International Reference Test Procedures," *Proceedings of First International Symposium on Penetration Testing, Orlando, FL*, A.A. Balkema Publishers, Rotterdam, Netherlands, 1988.
- (24) Van Vuuren, D. J., "Rapid Determination of CBR With the Portable Dynamic Cone Penetrometer," *The Rhodesian Engineer*, Vol 7, Number 5, Salisbury, Rhodesia, September 1968, pp. 852-854.

(25) Webster, S. L., Grau, R. H., and Williams, T. P., "Description and Application of Dual Mass Dynamic Cone Penetrometer," *Report GL-92-3*, Department of the Army, Washington DC, May 1992, p. 19.

(26) Webster, S. L., Brown, R. W., and Porter, J. R., "Force Projection Site Evaluation Using the Electric Cone Penetrometer (ECP) and the Dynamic Cone Penetrometer (DCP)," *Technical Report No. GL-94-17*, Air Force Civil Engineering Support Agency, U.S. Air Force, Tyndall Air Force Base, FL, April 1994.

(27) WinDCP 4.0: "Analysis and Classification of DCP Survey Data; User Manual and Software," 2000, Pretoria: Division of Roads and Transport Technology, CSIR, Divisional Publication: *DP-2000/5*.

